


Effects of nonstandard neutrino self-interactions and magnetic moment on collective Majorana neutrino oscillations

Oleg G. Kharlanov ^{*}

Faculty of Physics, Lomonosov Moscow State University, 1/2 Leninskie Gory, 119991 Moscow, Russia

Pavel I. Shustov 

*Space Research Institute of the Russian Academy of Sciences,
84/32 Profsoyuznaya Street, 117997 Moscow, Russia*



(Received 18 January 2021; accepted 7 April 2021; published 7 May 2021)

We derive the effective Hamiltonian describing collective oscillations of Majorana neutrinos with a transition magnetic moment, allowing for the presence of scalar and pseudoscalar nonstandard neutrino self-interactions (NSSIs). Using this Hamiltonian, we analyze new flavor instability channels of collective oscillations in a core-collapse supernova environment that open up in the presence of a small but nonzero neutrino magnetic moment. It turns out that, contrary to certain claims in the literature, within the minimally extended Standard Model (i.e., without NSSIs), no new instabilities arise within the linear order, nor do they produce any observable signatures in the neutrino flavor-energy spectra, at least for magnetic moments up to $10^{-15}\mu_B$ and quite realistic fields of the order of 10^{12} Gauss. On the other hand, in the presence of NSSIs, new fast and slow instabilities mixing neutrinos and antineutrinos appear, which show up in the spectra even for tiny magnetic moments of the order of $10^{-24}\mu_B$, leading to considerable distortions of the spectra and nonstandard spectral splits. We study sensitivity of collective oscillations to these, NSSI-induced instabilities in detail and discuss the observability of the NSSI couplings triggering them.

DOI: [10.1103/PhysRevD.103.095004](https://doi.org/10.1103/PhysRevD.103.095004)

I. INTRODUCTION

During the most violent phase of a core-collapse supernova explosion, emitted neutrinos carry away the lion's share of the explosion energy and turn out to be the first signal from a newborn supernova coming from its innermost regions [1,2]. An observation of supernova neutrinos could thus yield priceless information both on the physical processes at work during the explosion and on the physics of the neutrino itself in such an extreme environment, possibly unveiling signatures of certain beyond-Standard-Model (BSM) phenomena [3–7]. Indeed, thanks to the progress in experimental techniques of neutrino detection made since the SN 1987A event, modern neutrino observatories, as well as those planned to start operating in the coming years, should be able to yield a number of events quite sufficient to draw the neutrino energy spectra. For instance, for a 10 kpc-away explosion, the JUNO detector

would yield as many as several thousand events in both the neutrino and the antineutrino channels, including the inverse-beta-decay detection channel with an unprecedented energy resolution about 1% [8]. Inevitably though, the energy spectra thus observed would be a result of neutrino oscillations on the way from the supernova core (the proton-neutron star) to the detector, so, in order to “decipher” the spectra, one should be able to “rewind” these oscillations back to the stellar interior.

For a typical core-collapse supernova, the neutrino densities turn out to be so high next to their last scattering surface (also referred to as the neutrino sphere) that neutrino-neutrino forward scattering processes become important for the flavor evolution, ushering into the physics of collective neutrino oscillations [9]. This self-induced, nonlinear process shapes the flavor-energy spectra in the region deep under the Mikheev-Smirnov-Wolfenstein (MSW) resonance surface, i.e., where noncollective oscillations would be suppressed by a gigantic matter potential [10,11]. One of the main drivers of collective flavor transformations is the instabilities, which are intrinsically present in the nonlinear evolution equations on collective oscillations [9,12–17]. It has been identified, indeed, that a hierarchy of these instabilities, both in the linearized and fully nonlinear regimes, can lead to specific neutrino

^{*}kharlanov@physics.msu.ru

Published by the American Physical Society under the terms of the Creative Commons Attribution 4.0 International license. Further distribution of this work must maintain attribution to the author(s) and the published article's title, journal citation, and DOI. Funded by SCOAP³.

spectral features, such as the so-called spectral swaps (splits) and the behavior resembling turbulence [18–20].

New types of instabilities often arise when new degrees of freedom come into play. For example, fast instabilities show up beyond the so-called single-angle scheme [12,14–16,21]; lifting the assumption of translational invariance of the solution leads to turbulent flavor patterns breaking this invariance on a wide range of spatial scales [19,20,22]. In view of this, it seems appealing to analyze the effect of the neutrino anomalous magnetic moment [23], which mixes the two helicity states and thus doubles the number of nontrivially interacting degrees of freedom, on the spectrum of instabilities. This also sounds natural because of superstrong magnetic fields typical for collapsing stars. This problem has been studied in a number of papers, including the derivation of the effective Hamiltonian [6,24,25] and the impact on the flavor evolution within the single-angle [6,26] and multiangle frameworks [27]. Notably, the effective Hamiltonians derived/used in Refs. [24–27] and Ref. [6] are different in the self-interaction term and lead to drastically different flavor evolutions: in the latter case, new types of instabilities arise that strongly deform the neutrino flavor-energy spectra even for tiny values of the magnetic moment [6].

Certainly, it seems interesting not only to settle the question of the correct Hamiltonian, but rather to ask a more general question: are there any other factors producing neutrino flavor signatures in an interplay with the effects of a (tiny) neutrino magnetic moment? At least one answer to this question is discussed in the present paper. Namely, we study the effect of the so-called nonstandard neutrino self-interactions (NSSIs, see Refs. [28–30] for a review) on the collective flavor evolution of Majorana neutrinos triggered by the nonzero neutrino transition magnetic moment. Recently, NSSIs, i.e., four-fermion neutrino-neutrino interactions that are absent in the electroweak sector of the Standard Model, have attracted a lot of attention for being able to affect the observable neutrino spectra [31–35]. One can distinguish two classes of NSSIs, those with flavor-dependent V–A interactions and those with a non-V–A tensor structure of the four-fermion interaction. The NSSIs of the second class, specifically, those involving scalar $(\bar{\nu}\nu)^2$ and pseudoscalar $(\bar{\nu}\gamma_5\nu)^2$ terms, are especially interesting to us in our context, since, as we show below, their presence opens up a new instability channel in oscillations of Majorana neutrinos with a nonzero magnetic moment. It is worth admitting here that another instability channel due to scalar-pseudoscalar NSSIs has already been studied in Ref. [34]; however, the corresponding unstable modes do not mix the neutrino helicities and the nonvanishing magnetic moment is not crucial for their development.

According to our analysis which follows, it turns out that presence of a scalar-pseudoscalar NSSI violently deforms the neutrino spectra even for minuscule values of the

magnetic moment, at least down to $10^{-24}\mu_B$ for nonexaggerated stellar fields $B \sim 10^{12}$ Gauss, while in the absence of NSSIs (i.e., for the neutrino interactions within the Standard Model), the effect of the magnetic moment is virtually unobservable even for much greater magnetic moments. Moreover, certain NSSI signatures originating in collective oscillations deep inside the supernova, such as the anomalous neutrino-to-antineutrino number ratio, can be safely transported to the surface and further to the detector. This means that supernova neutrino spectra can be used to probe the presence of (pseudo)scalar NSSIs, possibly stemming from exchange of (pseudo)scalar BSM particles. The steps we take within our analysis of the NSSI-induced instabilities are presented in the following sections. Namely, in Sec. II, we rederive the Hamiltonian for collective Majorana neutrino oscillations with NSSIs and a nonzero neutrino magnetic moment and compare the no-NSSI case with the results of previous derivations. Further, in Sec. III, we carry out a linear stability analysis of our flavor evolution equations, also showing why in the absence of NSSIs, the effect of the magnetic moment should be small. Focusing then on the most interesting NSSI-induced unstable modes mixing the two neutrino helicities, we determine their growth rates, revealing fast and slow branches, as well as a specific intermediate, matter density dependent one. The linear analysis is accompanied by a full numerical simulation in Sec. IV, to study what happens beyond the linear stability regime and to determine the sensitivities of the spectra to the neutrino magnetic moment and the NSSI couplings. Section V summarizes the results obtained and discusses their possible generalizations. In the Appendix, several identities are proved or listed that we use in the derivation of the effective Hamiltonian in the presence of NSSIs.

II. EVOLUTION EQUATION FOR COLLECTIVE OSCILLATIONS IN THE PRESENCE OF NSSIs

Let us now settle the question of the effective Hamiltonian for collective oscillations of Majorana neutrinos with nonzero magnetic moment we mentioned above and, more importantly, derive the terms in this Hamiltonian that describe the scalar and pseudoscalar NSSIs. For that, let us derive the evolution equations for the neutrino flavor density matrix accounting for the forward scattering processes, starting from field theory. We use relativistic units $\hbar = c = 1$ throughout the paper.

We consider Majorana neutrinos in a small representative volume V , interacting with background electrons, protons, and neutrons, plus an external electromagnetic field $F_{\mu\nu}(x)$. After the electroweak symmetry is broken, the terms in the Lagrangian that contribute to neutrino forward scattering read [2,23,34,36]

$$\mathcal{L}_\nu = \mathcal{L}_{\text{vac}}^{(2)} + \mathcal{L}_{\text{mat}}^{(2)} + \mathcal{L}_{\text{AMM}}^{(2)} + \mathcal{L}_{\text{VA}}^{(4)} + \mathcal{L}_{\text{SP}}^{(4)}, \quad (1)$$

$$\mathcal{L}_{\text{vac}}^{(2)} = \frac{1}{2} \sum_{a=1}^{N_f} \bar{\nu}_a (i\gamma^\mu \partial_\mu - m_a) \nu_a, \quad (2)$$

$$\begin{aligned} \mathcal{L}_{\text{mat}}^{(2)} = & -G_F \sqrt{2} \bar{\nu}_f \gamma_L^\mu \nu_f \{ -\delta_{f,f'} [\bar{p} (2s_W^2 \gamma_\mu - \gamma_{\mu L}) p \\ & + \bar{n} \gamma_{\mu L} n] + \bar{e} [\delta_{f,f'} (2s_W^2 \gamma_\mu - \gamma_{\mu L}) + 2\delta_{f,e} \delta_{f',e} \gamma_{\mu L}] e \}, \end{aligned} \quad (3)$$

$$\mathcal{L}_{\text{AMM}}^{(2)} = -\frac{i}{4} \mathbf{m}_{ab} \bar{\nu}_a \sigma_{\mu\nu} F^{\mu\nu} \nu_b, \quad (4)$$

$$\mathcal{L}_{\text{VA}}^{(4)} = -\frac{G_F}{\sqrt{2}} : (\bar{\nu}_a \gamma_L^\mu \nu_a)^2 :, \quad (5)$$

$$\mathcal{L}_{\text{SP}}^{(4)} = -\frac{G_F}{4\sqrt{2}} \{ g_S : (\bar{\nu}_a \nu_a)^2 : + g_P : (\bar{\nu}_a \gamma_5 \nu_a)^2 : \}. \quad (6)$$

Here $\nu_a(x)$, $a = 1, \dots, N_f$, are the neutrino fields with Majorana masses m_a and $e(x)$, $p(x)$, $n(x)$ are the fields describing electrons, protons, and neutrons, respectively. The notations $\mathcal{L}_{\text{vac, mat, AMM}}^{(2)}$ versus $\mathcal{L}_{\text{VA, SP}}^{(4)}$ emphasize the quadratic and quartic dependence of these terms in the Lagrangian on the neutrino fields, respectively; these groups of terms will require different treatment when deriving the flavor evolution equations below. By definition, the neutrino fields obey Majorana constraints $\bar{\nu}_a(x) = \nu_a^\dagger(x)C$, where $C = -i\gamma^2\gamma^0$ is the charge conjugation matrix and the bar denotes a Dirac conjugate $\bar{\psi} \equiv \psi^\dagger\gamma^0$. The Dirac matrices $\gamma_L^\mu \equiv \gamma^\mu(1 - \gamma_5)/2$, $\sigma_{\mu\nu} \equiv \frac{1}{2}[\gamma_\mu, \gamma_\nu]$; $s_W \equiv \sin\theta_W$ is the sine of the weak mixing angle, and G_F is the Fermi constant; colons in Eqs. (5) and (6) denote normal ordering of field operators. The neutrino flavor states are defined via a Pontecorvo-Maki-Nakagawa-Sakata (PMNS) matrix [36,37] assumed to be unitary,

$$\nu_f(x) \equiv U_{fa} \nu_a(x), \quad \nu_a(x) \equiv U_{fa}^* \nu_f(x), \quad (7)$$

where the summation over the mass indices a, b, \dots and flavor indices f, f', \dots is assumed, the latter take on e, μ, τ values in the three-flavor case and e, x values in the two-flavor case. The electromagnetic interaction term (4) contains the neutrino magnetic moment matrix \mathbf{m}_{ab} , which is real and antisymmetric in the Majorana case, so that only transition magnetic moments are allowed [23]. Finally, the quartic terms (5), (6) describe the electroweak (V–A) and the nonstandard (scalar/pseudoscalar, SP) neutrino interactions, and the latter is parametrized by two dimensionless NSSI couplings $g_{S,P}$.

Within the forward-scattering approximation, i.e., while momentum-changing processes of the form $\nu_a(\mathbf{p}) \rightarrow \nu_b(\mathbf{p}')$, $\nu_a(\mathbf{p}) \rightarrow \bar{\nu}_b(\mathbf{p}')$ with $\mathbf{p}' \neq \mathbf{p}$ play a minor role, we can ignore coherent superpositions of different neutrino momentum states (while keeping track of coherent

superpositions of *mass* states due to oscillations). Accordingly, the neutrino state(s) $|\Phi\rangle$ we will consider below factorize into a infinite tensor product of state vectors $|\Phi_{\mathbf{p}}\rangle$, each of them describing neutrinos with a fixed momentum \mathbf{p} and belonging to the corresponding Fock space,

$$|\Phi\rangle = \otimes_{\mathbf{p}} |\Phi_{\mathbf{p}}\rangle, \quad (8)$$

$$|\Phi_{\mathbf{p}}\rangle = \sum_{A_1 \dots A_{N_{\mathbf{p}}}} C_{A_1 \dots A_{N_{\mathbf{p}}}}(\mathbf{p}) \hat{a}_{A_1 \mathbf{p}}^\dagger \dots \hat{a}_{A_{N_{\mathbf{p}}} \mathbf{p}}^\dagger |0_{\mathbf{p}}\rangle. \quad (9)$$

Here, for the sake of the calculations which will follow, we adopt a notation $A = (a\alpha)$, $B = (b\beta)$, ... for the creation operators $\hat{a}_{A\mathbf{p}}^\dagger$, with the Latin indices $a, b, \dots = 1, \dots, N_f$ denoting the neutrino mass states and the Greek ones $\alpha, \beta, \dots = \pm 1$ standing for the neutrino helicities (multiplied by two). As mentioned above, the state vector $|\Phi_{\mathbf{p}}\rangle$ describes neutrinos with momentum \mathbf{p} , whose total number $N_{\mathbf{p}} \in \{0, 1, \dots, 2N_f\}$ is limited due to the Pauli exclusion principle; moreover, in the forward scattering regime, these numbers are conserved for every individual \mathbf{p} and

$$\sum_A \hat{a}_{A\mathbf{p}}^\dagger \hat{a}_{A\mathbf{p}} \cdot |\Phi\rangle = N_{\mathbf{p}} |\Phi\rangle. \quad (10)$$

Thus, the time evolution of the neutrino state affects only the set of c -number-valued coefficients $C_{A_1 \dots A_{N_{\mathbf{p}}}}(\mathbf{p})$. It is much more convenient, however, to work with a $2N_f \times 2N_f$ neutrino flavor density matrix instead of these coefficients,

$$\rho_{AB}(\mathbf{p}) \equiv \langle \Phi | \hat{a}_{B\mathbf{p}}^\dagger \hat{a}_{A\mathbf{p}} | \Phi \rangle, \quad (11)$$

$$\frac{\partial \rho_{AB}(\mathbf{p})}{\partial t} = i \langle \Phi | [\hat{H}, \hat{a}_{B\mathbf{p}}^\dagger \hat{a}_{A\mathbf{p}}] | \Phi \rangle, \quad (12)$$

where \hat{H} is the Hamiltonian corresponding to the Lagrangian (1). Our task now is to transform Ehrenfest equation (12) into an effective von Neumann equation for the density matrix,

$$\begin{aligned} i \frac{\partial \rho_{AB}(\mathbf{p})}{\partial t} &= h_{AC}(\mathbf{p}) \rho_{CB}(\mathbf{p}) - h_{CB}(\mathbf{p}) \rho_{AC}(\mathbf{p}) \\ &\equiv [h(\mathbf{p}), \rho(\mathbf{p})]_{AB}, \end{aligned} \quad (13)$$

where $h(\mathbf{p})$ is the desired $2N_f \times 2N_f$ c -number matrix of the effective Hamiltonian, possibly depending on the density matrix ρ . In the derivation of the effective Hamiltonian, which follows, let us work in the Schrödinger picture and consider the contributions of the quadratic and quartic parts of \hat{H} (i.e., those arising from $\mathcal{L}_{\text{vac, mat, AMM}}^{(2)}$ and $\mathcal{L}_{\text{VA, SP}}^{(4)}$, respectively) separately.

In the ultrarelativistic approximation we are using, the Schrödinger-picture neutrino field operators $\nu_a(\mathbf{x})$ read

$$\nu_a(\mathbf{x}) = \frac{1}{\sqrt{V}} \sum_{\mathbf{p}, \alpha} \{ u_\alpha(\mathbf{p}) e^{i\mathbf{p}\cdot\mathbf{x}} \hat{a}_{a\alpha\mathbf{p}} + u_{-\alpha}(\mathbf{p}) e^{-i\mathbf{p}\cdot\mathbf{x}} \hat{a}_{a\alpha\mathbf{p}}^\dagger \},$$

$$a = 1, \dots, N_f, \quad (14)$$

where the 3-momentum $\mathbf{p} \in (2\pi/L)\mathbb{Z}^3$ is quantized in the normalization volume $V \equiv L \times L \times L$. The neutrino annihilation operators $\hat{a}_{a\alpha\mathbf{p}}$ enter together with the plane-wave solutions $u_\alpha(\mathbf{p}) e^{i\mathbf{p}\cdot\mathbf{x}}/\sqrt{V}$ describing particles with helicity $\alpha/2 = \pm 1/2$. In what follows, for brevity, we will refer to negative- and positive-helicity states as neutrino and antineutrino states, respectively, and also refer to $\alpha = \pm 1$ as the helicity values, instead of the rigorous helicities $\alpha/2 = \pm 1/2$. Some obvious expressions for the polarization bispinors $u_\alpha(\mathbf{p})$, as well as for their bilinear combinations we will need below, are listed in Appendix A.

The quadratic part of the Hamiltonian \hat{H} in the Ehrenfest equation (12), up to an insignificant multiple of the identity operator, can obviously be written as

$$\hat{H}^{(2)} = \sum_{C,D,\mathbf{q},\mathbf{r}} \lambda_{CD}(\mathbf{q}, \mathbf{r}) \hat{a}_{C\mathbf{q}}^\dagger \hat{a}_{D\mathbf{r}} + \hat{a} \hat{a} \text{ terms} + \hat{a}^\dagger \hat{a}^\dagger \text{ terms.} \quad (15)$$

The second and third terms produce vanishing contributions to the Ehrenfest equation, since $|\Phi\rangle$ possesses definite particle numbers $N_{\mathbf{p}}$ in all momentum modes. As for the particle number-conserving $\hat{a}^\dagger \hat{a}$ term, the corresponding contribution to the time derivative of the density matrix is evaluated straightforwardly:

$$\begin{aligned} i \frac{\partial \rho_{AB}(\mathbf{p})}{\partial t} &\supset -\langle \Phi | [\hat{H}^{(2)}, \hat{a}_{B\mathbf{p}}^\dagger \hat{a}_{A\mathbf{p}}] | \Phi \rangle \\ &= - \sum_{C,D,\mathbf{q},\mathbf{r}} \lambda_{CD}(\mathbf{q}, \mathbf{r}) \langle \Phi | \delta_{\mathbf{r}\mathbf{p}} \delta_{BD} \hat{a}_{C\mathbf{q}}^\dagger \hat{a}_{A\mathbf{p}} \\ &\quad - \delta_{\mathbf{q}\mathbf{p}} \delta_{AC} \hat{a}_{B\mathbf{p}}^\dagger \hat{a}_{D\mathbf{r}} | \Phi \rangle \\ &= [\lambda(\mathbf{p}, \mathbf{p}), \rho(\mathbf{p})]_{AB} \end{aligned} \quad (16)$$

and has the desired von Neumann structure (13) (the \supset sign means that quartic terms have been omitted on the rhs). Forward scattering clearly manifests itself in only the diagonal ($\mathbf{q} = \mathbf{r}$) entries of the coefficient function $\lambda(\mathbf{q}, \mathbf{r})$ affecting the evolution of the density matrix. Thus, to find the noncollective part of the desired effective Hamiltonian $h(\mathbf{p})$ in Eq. (13), one should simply list the three $\hat{a}^\dagger \hat{a}$ terms in $\hat{H}^{(2)}$ coming from the three Lagrangians $\mathcal{L}_{\text{vac}}^{(2)}$, $\mathcal{L}_{\text{mat}}^{(2)}$, and $\mathcal{L}_{\text{AMM}}^{(2)}$ describing the vacuum neutrino mixing and their interaction with matter and magnetic field. The first term gives nothing but a free Hamiltonian,

$$\hat{H}_{\text{vac}}^{(2)} = \sum_{\mathbf{q}, C} \sqrt{\mathbf{q}^2 + m_c^2} \hat{a}_{C\mathbf{q}}^\dagger \hat{a}_{C\mathbf{q}} = \sum_{\mathbf{q}, C, D} \lambda_{CD}^{\text{vac}}(\mathbf{q}, \mathbf{q}) \hat{a}_{C\mathbf{q}}^\dagger \hat{a}_{D\mathbf{q}}, \quad (17)$$

$$\begin{aligned} \lambda^{\text{vac}}(\mathbf{q}, \mathbf{q}) &= \begin{pmatrix} \sqrt{\mathbf{q}^2 + M^2} & 0 \\ 0 & \sqrt{\mathbf{q}^2 + M^2} \end{pmatrix} \\ &\approx |\mathbf{q}| \begin{pmatrix} \mathbb{1} & 0 \\ 0 & \mathbb{1} \end{pmatrix} + \begin{pmatrix} M^2/2|\mathbf{q}| & 0 \\ 0 & M^2/2|\mathbf{q}| \end{pmatrix}, \end{aligned} \quad (18)$$

where $(M^2)_{cd} = m_c^2 \delta_{cd}$ is the neutrino mass-squared matrix (in the mass basis here) and, as usual, the term proportional to the identity matrix does not contribute to the commutator in Eq. (16) and can be omitted. The matrix notation we have adopted in Eq. (18) and to be used hereinafter is as follows: the two block lines/columns of a $2N_f \times 2N_f$ matrix λ^{vac} correspond to the two helicities $\gamma, \delta = -1, +1$, following a pattern:

$$\rho \equiv \begin{pmatrix} \rho_{--} & \rho_{-+} \\ \rho_{+-} & \rho_{++} \end{pmatrix} \equiv \begin{pmatrix} \rho_{\nu\nu} & \rho_{\nu\bar{\nu}} \\ \rho_{\bar{\nu}\nu} & \rho_{\bar{\nu}\bar{\nu}} \end{pmatrix}. \quad (19)$$

In other words, the first and the second diagonal blocks describe neutrinos and antineutrinos, respectively, while the two off-diagonal blocks describe coherent mixtures of neutrinos and antineutrinos.

The matter (MSW) term in $\hat{H}^{(2)}$ can be retrieved by treating background matter and the corresponding e, p, n operators in the mean-field fashion:

$$\hat{H}_{\text{mat}}^{(2)} = - \int_V \mathcal{L}_{\text{mat}}^{(2)} d^3x \rightarrow G_F \sqrt{2} \langle \mathbb{J}_{ab}^\mu \rangle \int_V \bar{\nu}_a \gamma_\mu \nu_b d^3x. \quad (20)$$

The background matter current \mathbb{J}_{ab}^μ above is directly extracted from Eq. (3) and after averaging over neutral nonmoving nonmagnetized matter gives

$$\begin{aligned} \langle \mathbb{J}_{ab}^\mu \rangle &= -\delta_{ab} \langle \bar{p} (2s_W^2 \gamma^\mu - \gamma_L^\mu) p - \bar{e} (2s_W^2 \gamma^\mu - \gamma_L^\mu) e + \bar{n} \gamma_L^\mu n \rangle \\ &\quad + 2(\mathbb{P}_e)_{ab} \langle \bar{e} \gamma_L^\mu e \rangle \\ &= \delta_0^\mu \left\{ n_e (\mathbb{P}_e)_{ab} - \frac{n_n}{2} \delta_{ab} \right\}, \end{aligned} \quad (21)$$

where the projector onto the electron neutrino state $(\mathbb{P}_e)_{ab} \equiv U_{fa}^* \cdot \delta_{f,e} \delta_{f',e} \cdot U_{f'b}$ and $n_{e,n}$ are the electron and neutron number densities, respectively. Indeed, expectations of all axial vectors vanish, while for polar vectors, $\langle \bar{\ell} \gamma^\mu \ell \rangle = \delta_0^\mu n_\ell$, $\ell = e, p, n$. It remains now to directly substitute the neutrino operators (14) into (20) and extract the terms contributing to forward scattering [for the bilinear expressions of the form $\bar{u}(\dots)u$, see Appendix A]:

$$\begin{aligned} \hat{H}_{\text{mat}}^{(2)} &\supset G_F \sqrt{2} \sum_{\mathbf{q}, A, B} \langle \mathbb{J}_{ab}^0 \rangle \{ \bar{u}_\alpha(\mathbf{q}) \gamma_L^0 u_\beta(\mathbf{q}) \hat{a}_{A\mathbf{q}}^\dagger \hat{a}_{B\mathbf{q}} \\ &\quad - \bar{u}_{-\alpha}(\mathbf{q}) \gamma_L^0 u_{-\beta}(\mathbf{q}) \hat{a}_{B\mathbf{q}}^\dagger \hat{a}_{A\mathbf{q}} \} \\ &= \sum_{\mathbf{q}, A, B} \lambda_{AB}^{\text{mat}}(\mathbf{q}, \mathbf{q}) \hat{a}_{A\mathbf{q}}^\dagger \hat{a}_{B\mathbf{q}}, \end{aligned} \quad (22)$$

$$\begin{aligned} \lambda^{\text{mat}}(\mathbf{q}, \mathbf{q}) &= G_F \sqrt{2} \begin{pmatrix} \langle \mathbb{J}^0 \rangle & 0 \\ 0 & -\langle \mathbb{J}^0 \rangle^T \end{pmatrix} \\ &= G_F \sqrt{2} \begin{pmatrix} n_e \mathbb{P}_e - \frac{n_u}{2} \mathbb{1} & 0 \\ 0 & -n_e \mathbb{P}_e^T + \frac{n_u}{2} \mathbb{1} \end{pmatrix}. \end{aligned} \quad (23)$$

Finally, the magnetic moment term is evaluated in the same way giving

$$\begin{aligned} \hat{H}_{\text{AMM}}^{(2)} &= -\frac{i}{2} \mathbf{m}_{ab} \mathbf{B} \cdot \int_V \bar{\nu}_a \boldsymbol{\Sigma} \nu_b d^3x \\ &\supset \sum_{\mathbf{q}, A, B} \lambda_{AB}^{\text{AMM}}(\mathbf{q}, \mathbf{q}) \hat{a}_{A\mathbf{q}}^\dagger \hat{a}_{B\mathbf{q}}, \end{aligned} \quad (24)$$

$$\lambda^{\text{AMM}}(\mathbf{q}, \mathbf{q}) = -i\sqrt{2} \begin{pmatrix} 0 & (\boldsymbol{\zeta}_+(\mathbf{p}) \cdot \mathbf{B}) \mathbf{m} \\ (\boldsymbol{\zeta}_-(\mathbf{p}) \cdot \mathbf{B}) \mathbf{m} & 0 \end{pmatrix}, \quad (25)$$

where complex vectors $\boldsymbol{\zeta}_\pm(\mathbf{p}) = \frac{1}{\sqrt{2}} \chi_\mp^\dagger(\mathbf{p}) \boldsymbol{\sigma} \chi_\pm(\mathbf{p})$ are matrix elements of the Pauli matrices between states with opposite helicities (see Appendix A for the definition details and properties of these vectors).

Thus, we have found the noncollective part of the effective neutrino Hamiltonian to be $\lambda^{\text{vac}}(\mathbf{p}, \mathbf{p}) + \lambda^{\text{mat}}(\mathbf{p}, \mathbf{p}) + \lambda^{\text{AMM}}(\mathbf{p}, \mathbf{p})$, and we can now resort to the quartic terms in the neutrino Hamiltonian \hat{H} . These terms, after commutation with $\hat{a}_{B\mathbf{p}}^\dagger \hat{a}_{A\mathbf{p}}$ in the Ehrenfest equation (12), lead to quartic expectations of the form $\langle \Phi | \hat{a}^\dagger \hat{a}^\dagger \hat{a} \hat{a} | \Phi \rangle$. In order to close our system of equations on the density matrix, namely, to obtain (13), we will now

apply a kind of Wick's theorem and express such quartic expectations in terms of quadratic ones $\langle \Phi | \hat{a}_{B\mathbf{p}}^\dagger \hat{a}_{A\mathbf{p}} | \Phi \rangle = \rho_{AB}(\mathbf{p})$. Let us start from the contribution of the electro-weak Lagrangian (5) having a V–A structure and insert the corresponding Hamiltonian into Eq. (12):

$$\begin{aligned} i \frac{\partial \rho_{AB}(\mathbf{p})}{\partial t} &\supset i \left(\frac{\partial \rho_{AB}(\mathbf{p})}{\partial t} \right)_{\text{VA}} = -\frac{G_F}{\sqrt{2}} \int_V d^3x \\ &\quad \times \langle \Phi | [: (\bar{\nu}_c(\mathbf{x}) \gamma_L^\mu \nu_c(\mathbf{x}))^2 : , \hat{a}_{B\mathbf{p}}^\dagger \hat{a}_{A\mathbf{p}}] | \Phi \rangle. \end{aligned} \quad (26)$$

First of all, commutation with $\hat{a}_{B\mathbf{p}}^\dagger \hat{a}_{A\mathbf{p}}$ transforms creation and annihilation operators into creation and annihilation ones, respectively, i.e., it does not spoil the normal ordering. Thus, the commutator can safely be put inside the normal ordering, leading to an expectation of

$$\begin{aligned} &: [(\bar{\nu}_c(\mathbf{x}) \gamma_L^\mu \nu_c(\mathbf{x}))^2 , \hat{a}_{B\mathbf{p}}^\dagger \hat{a}_{A\mathbf{p}}] : \\ &= 2 : \bar{\nu}_c(\mathbf{x}) \gamma_L^\mu \nu_c(\mathbf{x}) [\bar{\nu}_d(\mathbf{x}) \gamma_{\mu L} \nu_d(\mathbf{x}) , \hat{a}_{B\mathbf{p}}^\dagger \hat{a}_{A\mathbf{p}}] :. \end{aligned} \quad (27)$$

Next, due to symmetries of bilinear expressions in Majorana fields (see, e.g., Ref. [2])

$$\begin{aligned} : \bar{\psi} \omega : &= : \bar{\omega} \psi : , \quad : \bar{\psi} \gamma_5 \omega : = : \bar{\omega} \gamma_5 \psi : , \\ : \bar{\psi} \gamma^\mu \omega : &= - : \bar{\omega} \gamma^\mu \psi : , \\ : \bar{\psi} \gamma^\mu \gamma_5 \omega : &= : \bar{\omega} \gamma^\mu \gamma_5 \psi : , \quad : \bar{\psi} \sigma_{\mu\nu} \omega : = - : \bar{\omega} \sigma_{\mu\nu} \psi : , \end{aligned} \quad (28)$$

the V–A currents can be replaced by axial vector ones, $\bar{\nu}_d(\mathbf{x}) \gamma_{\mu L} \nu_d(\mathbf{x}) = -\frac{1}{2} \bar{\nu}_d(\mathbf{x}) \gamma_\mu \gamma_5 \nu_d(\mathbf{x})$. Moreover, by virtue of the same symmetry properties, the latter one is a symmetric quadratic form in ν_d , and its commutator with $\hat{a}_{B\mathbf{p}}^\dagger \hat{a}_{A\mathbf{p}}$ leads to two identical terms, yielding $-\bar{\nu}_d(\mathbf{x}) \gamma_\mu \gamma_5 [\nu_d(\mathbf{x}) , \hat{a}_{B\mathbf{p}}^\dagger \hat{a}_{A\mathbf{p}}]$. As a result, the V–A contribution to the evolution equation for the density matrix takes the form

$$\begin{aligned} i \left(\frac{\partial \rho_{AB}(\mathbf{p})}{\partial t} \right)_{\text{VA}} &= -\frac{G_F}{\sqrt{2}} \int_V d^3x \langle \Phi | : \bar{\nu}_c(\mathbf{x}) \gamma^\mu \gamma_5 \nu_c(\mathbf{x}) \cdot \bar{\nu}_d(\mathbf{x}) \gamma_\mu \gamma_5 [\nu_d(\mathbf{x}) , \hat{a}_{B\mathbf{p}}^\dagger \hat{a}_{A\mathbf{p}}] : | \Phi \rangle \\ &= -\frac{G_F}{\sqrt{2V}} \int_V d^3x \langle \Phi | : \bar{\nu}_c(\mathbf{x}) \gamma^\mu \gamma_5 \nu_c(\mathbf{x}) \cdot \bar{\nu}_d(\mathbf{x}) \gamma_\mu \gamma_5 \{ \delta_{bd} e^{i\mathbf{p}\cdot\mathbf{x}} u_\beta(\mathbf{p}) \hat{a}_{A\mathbf{p}} - \delta_{ad} e^{-i\mathbf{p}\cdot\mathbf{x}} u_{-\alpha}(\mathbf{p}) \hat{a}_{B\mathbf{p}}^\dagger \} : | \Phi \rangle \\ &\equiv -\frac{G_F}{\sqrt{2V}} \int_V d^3x \langle \Phi | : \bar{\varphi} \gamma^\mu \gamma_5 \chi \cdot \bar{\psi} \gamma_\mu \gamma_5 \omega : | \Phi \rangle, \end{aligned} \quad (29)$$

where we have symbolically denoted $\varphi = \chi = \nu_c(\mathbf{x})$, $\psi = \nu_d(\mathbf{x})$, and $\omega = \delta_{bd} e^{i\mathbf{p}\cdot\mathbf{x}} u_\beta(\mathbf{p}) \hat{a}_{A\mathbf{p}} - \delta_{ad} e^{-i\mathbf{p}\cdot\mathbf{x}} u_{-\alpha}(\mathbf{p}) \hat{a}_{B\mathbf{p}}^\dagger$. A quartic expectation value we have encountered can now be (approximately) reduced to products of quadratic expectations, or contractions, by virtue of the Wick's theorem (see Appendix B for details)

$$\langle \Phi | : \bar{\varphi} \gamma^\mu \gamma_5 \chi \cdot \bar{\psi} \gamma_\mu \gamma_5 \omega : | \Phi \rangle \approx \overbrace{\bar{\varphi} \gamma^\mu \gamma_5 \chi} \cdot \overbrace{\bar{\psi} \gamma_\mu \gamma_5 \omega} + \overbrace{\bar{\varphi} \gamma^\mu \gamma_5 \chi \cdot \bar{\psi} \gamma_\mu \gamma_5 \omega} + \overbrace{\bar{\varphi} \gamma^\mu \gamma_5 \chi \cdot \bar{\psi} \gamma_\mu \gamma_5 \omega}, \quad (30)$$

where a contraction of two spinor fields $\overline{\varphi^i \chi^j} \equiv \langle \Phi | : \varphi^i \chi^j : | \Phi \rangle$, with $i, j = 1, 2, 3, 4$ numbering the components of a bispinor. To avoid using the index notation, however, we note that the second and the third terms in the above expression are equal due to (28) and apply the Fierz identity to them [38], arriving at

$$\langle \Phi | : \overline{\varphi} \gamma^\mu \gamma_5 \chi \cdot \overline{\psi} \gamma_\mu \gamma_5 \omega : | \Phi \rangle \approx \overline{\overline{\varphi} \gamma^\mu \gamma_5 \chi} \cdot \overline{\overline{\psi} \gamma_\mu \gamma_5 \omega} + 2 \overline{\overline{\varphi} \omega} \cdot \overline{\overline{\psi} \chi} - 2 \overline{\overline{\varphi} \gamma_5 \omega} \cdot \overline{\overline{\psi} \gamma_5 \chi} + \overline{\overline{\varphi} \gamma^\mu \omega} \cdot \overline{\overline{\psi} \gamma_\mu \chi} + \overline{\overline{\varphi} \gamma^\mu \gamma_5 \omega} \cdot \overline{\overline{\psi} \gamma_\mu \gamma_5 \chi}. \quad (31)$$

Now, every one of these contractions is a sum of expectation values of the form $\langle \Phi | \hat{a}^\dagger \hat{a} | \Phi \rangle$, which are nothing but specific entries of the density matrix ρ , namely,

$$\begin{aligned} \overline{\overline{\varphi} \gamma^\mu \gamma_5 \chi} &= \frac{2}{V} \sum_{\mathbf{q}, c, \gamma} \gamma(1, \hat{\mathbf{q}}) \rho_{c\gamma, c\gamma}(\mathbf{q}) \\ &\equiv -\frac{2}{V} \sum_{\mathbf{q}} (1, \hat{\mathbf{q}}) \text{tr}(\rho(\mathbf{q}) \mathcal{G}), \end{aligned} \quad (32)$$

$$\overline{\overline{\psi} \gamma^\mu \gamma_5 \omega} = \frac{(1, \hat{\mathbf{p}})}{\sqrt{V}} (\beta - \alpha) \rho_{AB}(\mathbf{p}) \equiv \frac{(1, \hat{\mathbf{p}})}{\sqrt{V}} [\mathcal{G}, \rho(\mathbf{p})]_{AB}, \quad (33)$$

$$\overline{\overline{\psi} \chi} = \overline{\overline{\psi} \gamma_5 \chi} = 0, \quad (34)$$

$$\overline{\overline{\psi} \gamma^\mu \chi} = \frac{1}{V} \sum_{\mathbf{q}, \gamma} (1, \hat{\mathbf{q}}) \wp_{c\gamma, d\gamma}(\mathbf{q}), \quad (35)$$

$$\overline{\overline{\varphi} \gamma^\mu \gamma_5 \omega} = \frac{1}{V} \sum_{\mathbf{q}, \gamma} \gamma(1, \hat{\mathbf{q}}) \wp_{c\gamma, d\gamma}(\mathbf{q}), \quad (36)$$

$$\overline{\overline{\varphi} \gamma^\mu \omega} = \frac{(1, \hat{\mathbf{p}})}{\sqrt{V}} \{ \delta_{bd} \rho_{A, c\beta}(\mathbf{p}) + \delta_{ad} \rho_{c\alpha, B}(\mathbf{p}) \}, \quad (37)$$

$$\overline{\overline{\varphi} \gamma^\mu \gamma_5 \omega} = \frac{(1, \hat{\mathbf{p}})}{\sqrt{V}} \{ \beta \delta_{bd} \rho_{A, c\beta}(\mathbf{p}) - \alpha \delta_{ad} \rho_{c\alpha, B}(\mathbf{p}) \}. \quad (38)$$

The above identities are obtained in a straightforward way from the neutrino operator (14) and the bilinears (A6)–(A11). In the first two identities, we have introduced a matrix distinguishing neutrinos and antineutrinos,

$$\mathcal{G} \equiv \begin{pmatrix} \mathbb{1} & 0 \\ 0 & -\mathbb{1} \end{pmatrix}, \quad \mathcal{G}_{c\gamma, d\delta} = -\gamma \delta_{cd} \delta_{\gamma\delta}, \quad (39)$$

while another matrix featuring in identities (35) and (36) is a difference between the density matrix and the charge conjugate of its transpose

$$\begin{aligned} \wp_{c\gamma, d\delta}(\mathbf{q}) &\equiv \rho_{c\gamma, d\delta}(\mathbf{q}) - \rho_{d-\delta, c-\gamma}(\mathbf{q}), \\ \wp(\mathbf{q}) &= \rho(\mathbf{q}) - \rho^{cT}(\mathbf{q}), \end{aligned} \quad (40)$$

$$\rho^c \equiv \mathcal{C} \rho \mathcal{C}, \quad \mathcal{C} \equiv \begin{pmatrix} 0 & \mathbb{1} \\ \mathbb{1} & 0 \end{pmatrix}. \quad (41)$$

The charge conjugation, as defined here, simply swaps the neutrino lines/columns with the antineutrino lines/columns of the density matrix.

Finally, after substituting the contractions listed above into the Fierz transformed Wick's theorem (31) and using the latter expression in the Ehrenfest equation (29), we obtain a contribution to the evolution of neutrino density matrix due to electroweak neutrino-neutrino interactions:

$$i \left(\frac{\partial \rho(\mathbf{p})}{\partial t} \right)_{\text{VA}} = [h_{\text{self}}^{\text{VA}}(\mathbf{p}), \rho(\mathbf{p})], \quad (42)$$

$$h_{\text{self}}^{\text{VA}}(\mathbf{p}) = \frac{G_{\text{F}} \sqrt{2}}{V} \sum_{\mathbf{q}} (1 - \hat{\mathbf{p}} \cdot \hat{\mathbf{q}}) \{ \text{tr}(\rho(\mathbf{q}) \mathcal{G}) \mathcal{G} + \wp^{\text{diag}}(\mathbf{q}) \}. \quad (43)$$

The $\wp^{\text{diag}}(\mathbf{q})$ matrix above is a block-diagonal part of $\wp(\mathbf{q})$:

$$\begin{aligned} \wp &\equiv \begin{pmatrix} \wp_{\nu\nu} & \wp_{\nu\bar{\nu}} \\ \wp_{\bar{\nu}\nu} & \wp_{\bar{\nu}\bar{\nu}} \end{pmatrix}, \\ \wp^{\text{diag}} &\equiv \frac{1}{2} (\wp + \mathcal{G} \wp \mathcal{G}) = \begin{pmatrix} \wp_{\nu\nu} & 0 \\ 0 & \wp_{\bar{\nu}\bar{\nu}} \end{pmatrix}. \end{aligned} \quad (44)$$

It is now time to find the term in the evolution equation coming from the scalar (S) and pseudoscalar (P) nonstandard neutrino interactions. This is done following exactly the same steps as in the V–A interaction case, but starting from Lagrangian (6). Namely, the S/P contribution to the time derivative of the density matrix reads

$$i \left(\frac{\partial \rho_{AB}(\mathbf{p})}{\partial t} \right)_{\text{SP}} = -\frac{G_F}{\sqrt{2V}} \int_V d^3x \langle \Phi | : g_S \bar{\varphi} \chi \cdot \bar{\psi} \omega + g_P \bar{\varphi} \gamma_5 \chi \cdot \bar{\psi} \gamma_5 \omega : | \Phi \rangle, \quad (45)$$

and after applying the Wick's theorem, we arrive at

$$i \left(\frac{\partial \rho_{AB}(\mathbf{p})}{\partial t} \right)_{\text{SP}} = -\frac{G_F}{\sqrt{2V}} \int_V d^3x \left\{ g_S \left(\overline{\varphi \chi} \cdot \overline{\psi \omega} + 2 \overline{\varphi \chi} \cdot \overline{\psi \omega} \right) + g_P \left(\overline{\varphi \gamma_5 \chi} \cdot \overline{\psi \gamma_5 \omega} + 2 \overline{\varphi \gamma_5 \chi} \cdot \overline{\psi \gamma_5 \omega} \right) \right\}. \quad (46)$$

Note that the first contractions in each of the two parentheses vanish due to Eq. (A6). For the second contractions, we use the Fierz identity [38], omitting the vanishing scalar and pseudoscalar terms in it (34), and arrive at

$$i \left(\frac{\partial \rho_{AB}(\mathbf{p})}{\partial t} \right)_{\text{SP}} = \frac{G_F}{\sqrt{2V}} \int_V d^3x \left\{ g_- \overline{\varphi \gamma^\mu \omega} \cdot \overline{\psi \gamma_\mu \chi} - g_- \overline{\varphi \gamma^\mu \gamma_5 \omega} \cdot \overline{\psi \gamma_\mu \gamma_5 \chi} + \frac{g_+}{2} \overline{\varphi \sigma^{\mu\nu} \omega} \cdot \overline{\psi \sigma_{\mu\nu} \chi} \right\}, \quad (47)$$

where $g_\pm \equiv (g_S \pm g_P)/2$. In fact, the vector and the axial vector terms have already been evaluated above, so that it remains only to evaluate the tensor one:

$$\frac{1}{2} \overline{\varphi \sigma^{\mu\nu} \omega} \cdot \overline{\psi \sigma_{\mu\nu} \chi} = \overline{\varphi \Sigma \omega} \cdot \overline{\psi \Sigma \chi} + \overline{\varphi \alpha \omega} \cdot \overline{\psi \alpha \chi}, \quad (48)$$

$$\overline{\psi \Sigma \chi} = \frac{\sqrt{2}}{V} \sum_{\mathbf{q}, \gamma} \zeta_\gamma(\mathbf{q}) \wp_{c\gamma, d-\gamma}(\mathbf{q}), \quad (49)$$

$$\overline{\psi \alpha \chi} = \frac{\sqrt{2}}{V} \sum_{\mathbf{q}, \gamma} \gamma \zeta_\gamma(\mathbf{q}) \wp_{c\gamma, d-\gamma}(\mathbf{q}), \quad (50)$$

$$\overline{\varphi \Sigma \omega} = \sqrt{\frac{2}{V}} \{ \delta_{bd} \zeta_\beta(\mathbf{p}) \rho_{A, c-\beta}(\mathbf{p}) + \delta_{ad} \zeta_{-\alpha}(\mathbf{p}) \rho_{c-\alpha, B}(\mathbf{p}) \}, \quad (51)$$

$$\overline{\varphi \alpha \omega} = \sqrt{\frac{2}{V}} \{ \delta_{bd} \beta \zeta_\beta(\mathbf{p}) \rho_{A, c-\beta}(\mathbf{p}) - \delta_{ad} \alpha \zeta_{-\alpha}(\mathbf{p}) \rho_{c-\alpha, B}(\mathbf{p}) \}. \quad (52)$$

Again, working in the same way as we did in the case of V-A interaction, we transform Eq. (47) into

$$i \left(\frac{\partial \rho(\mathbf{p})}{\partial t} \right)_{\text{SP}} = [h_{\text{self}}^{\text{SP}}(\mathbf{p}), \rho(\mathbf{p})], \quad (53)$$

$$h_{\text{self}}^{\text{SP}}(\mathbf{p}) = \frac{G_F \sqrt{2}}{V} \sum_{\mathbf{q}} (1 - \hat{\mathbf{p}} \cdot \hat{\mathbf{q}}) \{ g_- (\wp^{\text{diag}}(\mathbf{q}))^T + g_+ e^{i\Gamma(\hat{\mathbf{p}}, \hat{\mathbf{q}})} \mathcal{G} (\wp^{\text{offdiag}}(\mathbf{q}))^T \}, \quad (54)$$

where we have expressed the scalar products $\zeta_\pm(\mathbf{p}) \cdot \zeta_\pm(\mathbf{p}) = e^{\pm i\Gamma(\hat{\mathbf{p}}, \hat{\mathbf{q}})} (1 - \hat{\mathbf{p}} \cdot \hat{\mathbf{q}})/2$ in terms of a single complex phase $\Gamma(\hat{\mathbf{p}}, \hat{\mathbf{q}})$ (see Appendix A). The block-off-diagonal part of the matrix above is defined analogously to Eq. (44):

$$\wp^{\text{offdiag}} \equiv \frac{1}{2} (\wp - \mathcal{G} \wp \mathcal{G}) = \begin{pmatrix} 0 & \wp_{\nu\bar{\nu}} \\ \wp_{\bar{\nu}\nu} & 0 \end{pmatrix}, \quad \wp = \wp^{\text{diag}} + \wp^{\text{offdiag}}. \quad (55)$$

In fact, this block-off-diagonal part anticommutes with \mathcal{G} , which underpins Hermiticity of the g_+ part of the Hamiltonian. Further, the complex phase $\Gamma(\hat{\mathbf{p}}, \hat{\mathbf{q}})$ comes from the phases included in the helicity eigenstates $\chi_{\pm}(\mathbf{p})$, $\chi_{\pm}(\mathbf{q})$; one would therefore like to rephase helicity eigenstates, thus getting rid of the $e^{i\Gamma\mathcal{G}}$ term in the NSSI Hamiltonian. However, this is impossible to achieve on the whole Bloch sphere $\hat{\mathbf{p}}, \hat{\mathbf{q}} \in S^2$, since the parallel transport of the helicity eigenstates across this sphere is characterized with a nonzero Berry curvature [39].

As we observe, both in the electroweak and the non-standard scalar-pseudoscalar case, the time derivative of the neutrino flavor density matrix $\rho(\mathbf{p})$ can be cast into a von Neumann form (13), i.e., a form of a commutator with a Hermitian matrix $h(\mathbf{p})$. Writing down all the contributions to this time derivative together [see Eqs. (18), (23), (25), (43), (54)], we finally arrive at the desired evolution equation on ρ :

$$i\frac{\partial\rho(\mathbf{p})}{\partial t} = [h(\mathbf{p}), \rho(\mathbf{p})], \quad (56)$$

$$\begin{aligned} h(\mathbf{p}) &= h_{\text{vac}}(\mathbf{p}) + h_{\text{mat}} + h_{\text{AMM}}(\mathbf{p}) + h_{\text{self}}(\mathbf{p}) \\ &\equiv \frac{1}{2|\mathbf{p}|} \begin{pmatrix} M^2 & 0 \\ 0 & M^2 \end{pmatrix} + G_F\sqrt{2} \begin{pmatrix} n_e \mathbb{P}_e - \frac{n_n}{2} \mathbb{1} & 0 \\ 0 & -n_e \mathbb{P}_e + \frac{n_n}{2} \mathbb{1} \end{pmatrix} - i \begin{pmatrix} 0 & \mathbf{m} \cdot \mathbf{B}_{\perp}(\mathbf{p}) \\ \mathbf{m} \cdot \mathbf{B}_{\perp}^*(\mathbf{p}) & 0 \end{pmatrix} \\ &\quad + \frac{G_F\sqrt{2}}{V} \sum_{\mathbf{q}} (1 - \hat{\mathbf{p}} \cdot \hat{\mathbf{q}}) \{ \text{tr}(\rho(\mathbf{q})\mathcal{G})\mathcal{G} + \wp^{\text{diag}}(\mathbf{q}) + g_-(\wp^{\text{diag}}(\mathbf{q}))^T + g_+ e^{i\Gamma(\hat{\mathbf{p}}, \hat{\mathbf{q}})\mathcal{G}}(\wp^{\text{offdiag}}(\mathbf{q}))^T \}, \end{aligned} \quad (57)$$

where one can show that $B_{\perp}(\mathbf{p}) \equiv \sqrt{2}\zeta_+(\mathbf{p}) \cdot \mathbf{B}$ is indeed a complex number with the absolute value equal to the strength of the magnetic field across the neutrino momentum (in accordance with the notation we use). The equations of motion possess a gauge freedom with respect to rephasing the helicity eigenstates,

$$\rho(\mathbf{p}) \rightarrow e^{i\gamma(\hat{\mathbf{p}})\mathcal{G}/2} \rho(\mathbf{p}) e^{-i\gamma(\hat{\mathbf{p}})\mathcal{G}/2}, \quad (58)$$

$$\begin{aligned} B_{\perp}(\mathbf{p}) &\rightarrow B_{\perp}(\mathbf{p}) e^{i\gamma(\hat{\mathbf{p}})}, \\ \Gamma(\hat{\mathbf{p}}, \hat{\mathbf{q}}) &\rightarrow \Gamma(\hat{\mathbf{p}}, \hat{\mathbf{q}}) + \gamma(\hat{\mathbf{p}}) + \gamma(\hat{\mathbf{q}}), \end{aligned} \quad (59)$$

where $\gamma(\hat{\mathbf{p}})$ is a real function on a sphere describing the gauge transformation. This transformation virtually tunes the relative phases of neutrino and antineutrino states and becomes trivial for a block-diagonal density matrix, i.e., if neutrinos do not coherently mix with antineutrinos.

It is also instructive here to emphasize that the off-diagonal blocks of $\rho(\mathbf{p})$ do not behave as scalars under rotations. Indeed, the spinor representation of a rotation $R(\mathbf{n}, \vartheta) \in SO(3)$ around the \mathbf{n} axis on ϑ radians has the form

$$\hat{U}(R(\mathbf{n}, \vartheta)) \nu_a(\mathbf{x}, t) \hat{U}^{\dagger}(R(\mathbf{n}, \vartheta)) = e^{i\mathbf{n} \cdot \Sigma \vartheta/2} \nu_a(R(\mathbf{n}, \vartheta) \mathbf{x}, t), \quad (60)$$

from which one readily obtains the transformation of the neutrino annihilation operators

$$\hat{U}(R(\mathbf{n}, \vartheta)) \hat{a}_{A\mathbf{p}} \hat{U}^{\dagger}(R(\mathbf{n}, \vartheta)) = e^{i\alpha \Xi(\mathbf{p}, \mathbf{n}, \vartheta)} \hat{a}_{A, R(\mathbf{n}, \vartheta) \mathbf{p}}, \quad (61)$$

where the phase Ξ is connected with the complex phases chosen in the helicity eigenstates, $e^{i\mathbf{n} \cdot \sigma \vartheta/2} \chi_{\pm}(R(\mathbf{n}, \vartheta) \mathbf{p}) \equiv e^{\pm i\Xi(\mathbf{p}, \mathbf{n}, \vartheta)} \chi_{\pm}(\mathbf{p})$. Now, if one rotates the neutrino state, $|\Phi\rangle \rightarrow |\Phi'\rangle = \hat{U}^{\dagger}(R(\mathbf{n}, \vartheta)) |\Phi\rangle$, the density matrix $\rho_{AB}(\mathbf{p}) = \langle \Phi | \hat{a}_{B\mathbf{p}}^{\dagger} \hat{a}_{A\mathbf{p}} | \Phi \rangle$ will transform as

$$\rho(\mathbf{p}) \rightarrow \rho'(\mathbf{p}) = e^{-i\Xi(\mathbf{p}, \mathbf{n}, \vartheta)\mathcal{G}} \rho(R(\mathbf{n}, \vartheta) \mathbf{p}) e^{i\Xi(\mathbf{p}, \mathbf{n}, \vartheta)\mathcal{G}}. \quad (62)$$

Just like in the case of a gauge transformation, the diagonal blocks are left intact, while the off-diagonal ones get rephased. In particular, one can demonstrate that for the neutrino-antineutrino block,

$$\rho'_{\nu\bar{\nu}}(\mathbf{p}) \zeta_{-}(\mathbf{p}) = \rho_{\nu\bar{\nu}}(R\mathbf{p}) R^{-1} \zeta_{-}(R\mathbf{p}), \quad (63)$$

i.e., its product with the ζ_{-} vector transforms as a vector field without additional phases. As a result, for an isotropic neutrino gas ($\rho'(\mathbf{p}) = \rho(\mathbf{p})$), the above equation tells us that $\rho_{\nu\bar{\nu}}(\mathbf{p}) \zeta_{-}(\mathbf{p})$ is a spherically symmetric vector field. However, because $\mathbf{p} \cdot \zeta_{-}(\mathbf{p}) = 0$ (see Appendix A), this requires $\rho_{\nu\bar{\nu}}(\mathbf{p}) = 0$. That is, nontrivial neutrino-antineutrino mixing violates isotropy, so the NSSI Hamiltonian (57) loses its g_+ term when applied to an isotropic neutrino gas.

In the next two sections, we will study the effect of the nontrivial neutrino NSSIs on the flavor evolution in the neutrino bulb model using the so-called single-angle scheme [9]. To obtain the corresponding evolution equations, we focus on stationary processes with propagating neutrinos and make a replacement transforming the von Neumann equation (13) into a quantum Liouville equation:

$$\frac{\partial \rho(\mathbf{p}; t)}{\partial t} \rightarrow \left(\frac{\partial}{\partial t} + \hat{\mathbf{p}} \cdot \frac{\partial}{\partial \mathbf{x}} \right) \rho(\mathbf{p}, \mathbf{x}) = (\hat{\mathbf{p}} \cdot \nabla) \rho(\mathbf{p}, \mathbf{x}). \quad (64)$$

Next, construction of the single-angle scheme should include introduction of the so-called geometric factor $\mathcal{D}(r/R_\nu)$, (partially) accounting for the nonspherically symmetric distribution of the neutrino numbers far from the neutrino sphere; even in the Standard-Model case, there exist several versions of it [9,18,40]. In our case, since the same factor $1 - \hat{\mathbf{p}} \cdot \hat{\mathbf{q}}$ appears in front of both the electroweak and NSSI g_- terms in the collective part of the Hamiltonian (57), it is natural to equip their single-angle counterparts with the same geometric factor. Regarding the g_+ term having an extra $e^{i\Gamma(\hat{\mathbf{p}} \cdot \hat{\mathbf{q}})\mathcal{G}}$ factor, the same may not be the case, however, we will keep the same geometric factor, qualitatively relying upon the argument that far from the neutrino sphere the solid angle spanned by the neutrino momenta \mathbf{q} is small and one can rephase the helicity eigenstates within it to approximately eliminate the phase factor $e^{i\Gamma\mathcal{G}}$. A more rigorous discussion of the geometric factor for the g_+ term of the Hamiltonian is to be given elsewhere.

With these points in mind, we can now write down the evolution equations of the single-angle scheme. Namely, in the flavor basis and the two-flavor approximation, a neutrino with energy E , escaping the protoneutron star radially from its neutrino sphere $r = R_\nu$ outwards, is described by equations

$$i \frac{\partial \rho_E(r)}{\partial r} = [h_E(r), \rho_E(r)], \quad (65)$$

$$h_E(r) = h_{\text{vac},E} + h_{\text{mat}}(r) + h_{\text{AMM}}(r) + h_{\text{self}}(r),$$

$$h_{\text{vac},E} = \frac{\eta \Delta m^2}{4E} \begin{pmatrix} \mathbb{M} & 0 \\ 0 & \mathbb{M} \end{pmatrix}, \quad \mathbb{M} \equiv \begin{pmatrix} -\cos 2\theta & \sin 2\theta \\ \sin 2\theta & \cos 2\theta \end{pmatrix}, \quad (66)$$

$$h_{\text{mat}}(r) = G_F \sqrt{2} \text{diag} \left(n_e(r) - \frac{n_n(r)}{2}, -\frac{n_n(r)}{2}, -n_e(r) + \frac{n_n(r)}{2}, \frac{n_n(r)}{2} \right), \quad (67)$$

$$h_{\text{AMM}}(r) = \begin{pmatrix} 0 & \mu_{12} B_\perp(r) \sigma_2 \\ \mu_{12} B_\perp^*(r) \sigma_2 & 0 \end{pmatrix}, \quad (68)$$

$$h_{\text{self}}(r) = G_F \sqrt{2} \mathcal{D} \left(\frac{r}{R_\nu} \right) n_\nu(r) \int_0^\infty dE' \{ \text{tr}(\rho_{E'}(r) \mathcal{G}) \mathcal{G} + \wp_{E'}^{\text{diag}}(r) + g_- (\wp_{E'}^{\text{diag}}(r))^T + g_+ (\wp_{E'}^{\text{offdiag}}(r))^T \}, \quad (69)$$

where Δm^2 is the mass squared difference, $\eta = \pm 1$ marks the normal/inverted mass hierarchy, θ is the vacuum mixing

angle, and μ_{12} is the transition magnetic moment (note that the diagonal entries $\mu_{11} = \mu_{22} = 0$ for Majorana neutrinos [23]); for brevity, we use the same notation ρ for the density matrix in the flavor basis. To get rid of additional factors, we have renormalized the density matrix so that

$$\int_0^\infty \text{tr} \rho_E(r) dE = 1; \quad (70)$$

after such a renormalization, the total neutrino number density $n_\nu(r)$ appears in the nonlinear collective term. Note also that in the two-flavor case, a nontrivial Majorana phase can be eliminated from all terms but the g_- NSSI term in the self-interaction (69) by a gauge transformation (58) (for details, see Appendix C). Thus, technically, the g_- term in (69) should also contain a Majorana phase, however, we are not focusing on this term further and thus limit ourselves to a simplified expression ignoring it.

The initial condition for the above system of equations is usually placed at the neutrino sphere, where different neutrino flavors/helicities are assumed to be thermalized with well-defined energy spectra:

$$\rho_E(R_\nu) = \text{diag}(s_{\nu_e}(E), s_{\nu_x}(E), s_{\bar{\nu}_e}(E), s_{\bar{\nu}_x}(E)), \quad (71)$$

with the normalization convention (70) requiring that

$$\int_0^\infty (s_{\nu_e}(E) + s_{\nu_x}(E) + s_{\bar{\nu}_e}(E) + s_{\bar{\nu}_x}(E)) dE = 1. \quad (72)$$

Equations similar to the above ones for collective oscillations of Majorana neutrinos have been derived earlier in a number of contexts. First of all, V–A neutrino-neutrino interactions were included into the effective Hamiltonian in Ref. [24], allowing for a nontrivial structure of this interaction in the flavor space. The result we obtained here agrees with Ref. [24] in the absence of nonstandard interactions ($g_\pm = 0$). In a recent paper [34], the collective NSSI Hamiltonian was derived in the absence of the neutrino magnetic moment. One also observes agreement of the matrix structure of our effective Hamiltonian with this paper for $\mu_{12} = 0$, however, our derivation goes qualitatively beyond this special case. Namely, interaction with the external magnetic field via the magnetic moment introduces mixing between neutrinos and antineutrinos, so that their states cannot be described by two $N_f \times N_f$ density matrices anymore, but a single $2N_f \times 2N_f$ matrix is necessary to refer to both neutrino and antineutrino flavors and their coherent mixtures. In fact, in the $\mu_{12} = 0$ (or $\mathbf{B} = 0$) case, our density matrix becomes block diagonal and its $\rho_{\nu\nu}$ and $\rho_{\bar{\nu}\bar{\nu}}$ blocks representing neutrinos and antineutrinos, respectively, do obey the evolution equations of the form [34].

In fact, careful comparison of the coefficient in front of the g_- NSSI term in our Hamiltonian (57) with Ref. [34]

reveals a twofold discrepancy: our result is 2 times greater. We have analyzed the two derivations and reckon that the discrepancy comes from the very method, rather than from a mistake in the calculations. The authors of Ref. [34] introduce a mean-field Hamiltonian \mathcal{H}_{MF} by reducing quartic neutrino field products to partially contracted quadratic ones, analogously to our Wick's theorem (46), and then use these quadratic operators in the effective evolution equation for the density matrix. In particular, being written in the notation we are using here, their Eq. (9) with $\alpha = \beta = a, \xi = \eta = b$ virtually claims that $:\bar{\nu}_a \nu_a \bar{\nu}_b \nu_b: \approx 2 \overbrace{\bar{\nu}_a \gamma_L^\mu \nu_b}^{\text{contracted}} : \bar{\nu}_a \gamma_{\mu L} \nu_b :$, which can be transformed into $\overbrace{\bar{\nu}_a \nu_a}^{\text{contracted}} : \bar{\nu}_b \nu_b : + : \bar{\nu}_a \nu_a \overbrace{\bar{\nu}_b \nu_b}^{\text{contracted}} : + : \bar{\nu}_a \nu_a \bar{\nu}_b \nu_b :$ using the Fierz identity. However, even though the expectation of this quadratic operator coincides with $\langle \Phi | : \bar{\nu}_a \nu_a \bar{\nu}_b \nu_b : | \Phi \rangle$, this does not apply to its commutator with $\hat{a}_{Bp}^\dagger \hat{a}_{Ap}$ one needs in the evolution equation (12): contracted operators are c -numbers and do not contribute to the commutator, while in Eq. (12) all four neutrino operators in $\bar{\nu}_a \nu_a \bar{\nu}_b \nu_b$ do contribute. Roughly speaking, a mean-field expression for a quartic Hamiltonian $\mathcal{H}(\nu) = g\nu^4$ should come from its quadratic part around the mean value $\langle \nu \rangle$, i.e., $\mathcal{H}_{\text{MF}} = \mathcal{H}''(\langle \nu \rangle)(\delta\nu)^2/2 = 6g(\nu)^2(\delta\nu)^2$, where $\delta\nu \equiv \nu - \langle \nu \rangle$; this expression features six terms, in contrast to the three terms assumed in Ref. [34]. In view of the above, we are inclined to treat our g_- coefficient in the Hamiltonian (57) as correct.

Next, we should also mention two papers [6] by de Gouvêa and Shalgar, in which the single-angle scheme for collective oscillations of Majorana neutrinos was analyzed in the $\mu_{12} \neq 0$ case. The papers analyzed the electroweak (V–A) four-fermion neutrino interaction, arriving at the neutrino self-interaction Hamiltonian of the form

$$h_{\text{self}}^{(\text{dGS})}(r) = G_F \sqrt{2} \mathcal{D} \left(\frac{r}{R_\nu} \right) n_\nu(r) \int_0^\infty dE' \{ \text{tr}(\rho_{E'}(r) \mathcal{G}) + \mathcal{G}_{\varphi_{E'}}(r) \mathcal{G} \}. \quad (73)$$

Note that such an interaction, in principle, includes off-diagonal blocks mixing neutrino and antineutrino states. In contrast, our collective Hamiltonian (69) does not have such blocks in the Standard-Model regime $g_\pm = 0$, even if the density matrix $\rho_E(r)$ contains them. As we will see below, this makes a considerable difference in the instability spectra of the two Hamiltonians and, as a result, in the evolution of the neutrino spectra in the magnetic field. In a nutshell, collective oscillations governed by interaction Hamiltonian (73) favor neutrino-antineutrino mixing due to the presence of nontrivial off-diagonal blocks, thus, a tiny mixing introduced into the system by the magnetic moment term is followed by its exponential growth due to instabilities; however, nothing like this occurs in the Standard-Model regime of our evolution equations (65), since the only source of neutrino-antineutrino mixing is the

(linear, noncollective) magnetic-moment term. In fact, one can also briefly explain the absence of off-diagonal blocks in our interaction Hamiltonian (69) in the Standard-Model regime: this Hamiltonian arises from the chiral limit of the V–A neutrino-neutrino interaction, which contains operators of the form $\bar{\psi} \gamma^\mu \chi, \bar{\psi} \gamma^\mu \gamma_5 \chi$ not mixing the two chiral components and thus neutrinos and antineutrinos [see Eq. (30)]. The corresponding terms in the interaction Hamiltonian are block diagonal [see Eqs. (32), (35), (36)]; the off-diagonal (neutrino-antineutrino) blocks appear once tensor interactions stemming from NSSIs come into play in Eq. (47). Suppression of chirality-mixing neutrino interactions within the Standard Model was also demonstrated in Ref. [25] and used in simulations of neutrino flavor evolution in Ref. [27].

In any case, despite the disagreement of the results of Ref. [6] with ours, as well as with the earlier Ref. [24], the Hamiltonian presented in the former paper can be treated as yet another type of NSSI containing nontrivial off-diagonal blocks. Moreover, it is spectacular that both the equations from Ref. [6] and our equations (65) conserve the block-diagonality property of the density matrix $\rho_E(r)$ along the trajectory, provided that $\mu_{12} = 0$ and that the initial condition $\rho_E(R_\nu)$ is block diagonal [e.g., the one we chose (71)]. In this case, $\rho = \rho^{\text{diag}} = \text{diag}(\rho_{\nu\nu}, \rho_{\bar{\nu}\bar{\nu}})$ and Hamiltonian (73) can be replaced by

$$h_{\text{self}}^{(\text{dGS})}(r) \rightarrow G_F \sqrt{2} \mathcal{D} \left(\frac{r}{R_\nu} \right) n_\nu(r) \times \int_0^\infty dE' \begin{pmatrix} \varphi_{\nu\nu, E'}(r) & 0 \\ 0 & \varphi_{\bar{\nu}\bar{\nu}, E'}(r) \end{pmatrix}, \quad (74)$$

which is nothing but the well-known expression within the Standard Model, also valid for Dirac neutrinos [9]. Our Hamiltonian (65) also takes the above conventional form, when additionally, $g_- = 0$, i.e., the scalar and the pseudo-scalar couplings are equal in the NSSI Lagrangian (6). If, in contrast, $g_- \neq 0$, then scalar-pseudoscalar NSSI terms are present in the diagonal blocks of the density matrix and survive in the $\mu_{12} = 0$ regime. Their effect has recently been analyzed in Ref. [34], revealing considerable deviations of the neutrino spectra from the predictions of the electroweak theory for nonvanishing g_- . As a result, constraints can be placed on the g_- coupling from the possible measurements of the neutrino spectra from a supernova, regardless of the magnitude of the neutrino magnetic moment.

Our Hamiltonian, however, contains another, “hidden” sector with the coupling g_+ , which produces no effect in the zero magnetic moment case. It is this coupling that is able to introduce block-off-diagonal terms into the self-interaction Hamiltonian (69), possibly leading to nontrivial evolution of neutrino-antineutrino mixing. In the special case $g_- = 0, g_+ = -1$, the corresponding interaction term takes a form resembling the Hamiltonian (73) from Ref. [6]:

$$h_{\text{self}}(r) = G_F \sqrt{2} \mathcal{D} \left(\frac{r}{R_\nu} \right) n_\nu(r) \int_0^\infty dE' \{ \text{tr}(\rho_{E'}(r) \mathcal{G}) \mathcal{G} \\ + \wp_{E'}^{\text{diag}}(r) - (\wp_{E'}^{\text{offdiag}}(r))^\top \}, \quad g_+ = -1 \quad (75)$$

(note that $\mathcal{G} \rho_{E'} \mathcal{G} = \wp_{E'}^{\text{diag}} - \wp_{E'}^{\text{offdiag}}$), yet, it differs in the transposition of the off-diagonal part of the density matrix. As we will see below, however, the transposition leads to qualitatively different effects, and we have to conclude that the interaction (73) introduced in Ref. [6] cannot originate from scalar/pseudoscalar four-fermion interactions of Majorana neutrinos.

Finally, we would like to mention that we briefly analyzed the case of Dirac neutrinos in our recent paper [26], where coherent mixing between two (anti)neutrino helicity states was introduced by the magnetic moment. It turns out that the corresponding interaction Hamiltonian is also block diagonal in the absence of NSSIs and, as a result, the effect of the magnetic moment on the neutrino spectra is suppressed, not being subject to instabilities. In the present paper, we are not focusing on Dirac neutrinos, and the analysis which follows will be restricted to the Majorana case.

III. LINEAR STABILITY ANALYSIS

Before making numerical simulations of the single-angle scheme in various scenarios, it is instructive to take a look at the linear stability of the evolution equations. Our specific interest here regards the effect of a small neutrino magnetic moment; the crucial question is whether it can trigger new types of neutrino flavor instabilities that are hidden in the $\mu_{12} = 0$ regime.

As we mentioned above, when $\mu_{12} = 0$ and the initial condition is of the form (71), the density matrix $\rho_E^{(0)}(r)$ retains its block-diagonal form during the whole evolution $r \geq R_\nu$. For such a matrix, the effect of a nonzero g_+ NSSI term is absent, while the effect of the block-diagonal g_- term was studied in a recent paper [34]. Namely, in that paper, it was shown that the g_- term is able to trigger instabilities even in the absence of neutrino magnetic moment. Now, on top of possibly nonzero g_\pm couplings, let us switch on an infinitesimal magnetic moment $\mu_{12} \rightarrow 0$ and write down the equations of motion linearized in this small μ_{12} quantity:

$$\frac{\partial \delta \rho_E}{\partial r} + i \left[h_{\text{vac},E} + h_{\text{mat}} + h_{\text{self}}^{(0)}, \delta \rho_E \right] + i \left[\delta h_{\text{self}}, \rho_E^{(0)} \right] = \mathcal{J}_E(r), \quad (76)$$

$$\mathcal{J}_E(r) \equiv -i [h_{\text{AMM}}(r), \rho_E^{(0)}(r)] = \mathcal{O}(\mu_{12}), \quad (77)$$

$$\rho_E(r) = \rho_E^{(0)}(r) + \delta \rho_E(r), \quad \delta \rho_E(R_\nu) = 0; \\ \delta \rho_E(r) = \mathcal{O}(\mu_{12}), \quad (78)$$

where $h_{\text{self}}^{(0)}$ is the neutrino-neutrino Hamiltonian calculated for the density matrix $\rho_E^{(0)}$ and δh_{self} is its variation resulting from a variation $\delta \rho_E$ of the density matrix. For both standard and nonstandard neutrino interaction terms, one can separate the block-diagonal and block-off-diagonal parts of the above equation:

$$\frac{\partial \delta \rho_E^{\text{diag}}}{\partial r} + i \left[h_{\text{vac},E} + h_{\text{mat}} + h_{\text{self}}^{(0)}, \delta \rho_E^{\text{diag}} \right] + i \left[\delta h_{\text{self}}^{\text{diag}}, \rho_E^{(0)} \right] = 0, \quad (79)$$

$$\frac{\partial \delta \rho_E^{\text{offdiag}}}{\partial r} + i \left[h_{\text{vac},E} + h_{\text{mat}} + h_{\text{self}}^{(0)}, \delta \rho_E^{\text{offdiag}} \right] \\ + i \left[\delta h_{\text{self}}^{\text{offdiag}}, \rho_E^{(0)} \right] = \mathcal{J}_E(r). \quad (80)$$

Indeed, $h_{\text{vac},E} + h_{\text{mat}} + h_{\text{self}}^{(0)}$ is a block-diagonal matrix and so commutation with it does not mix the diagonal with off-diagonal contributions; the same applies to commutation with $\rho_E^{(0)}$; finally, the ‘‘source’’ term \mathcal{J}_E is purely block-off-diagonal because of the form of h_{AMM} . Note also that block-diagonal and block-off-diagonal parts of δh_{self} are determined by the corresponding parts of $\delta \rho_E$, so that evolutions of $\delta \rho_E^{\text{diag}}(r)$ and $\delta \rho_E^{\text{offdiag}}(r)$, defined by the two above equations, do indeed decouple in the linear regime. Technically, this means that one can search for block-diagonal and block-off-diagonal unstable modes separately.

If one sets g_+ to zero, i.e., turns off the block-off-diagonal part of the interaction, then the second equation becomes

$$\frac{\partial \delta \rho_E^{\text{offdiag}}}{\partial r} + i \left[h_{\text{vac},E} + h_{\text{mat}} + h_{\text{self}}^{(0)}, \delta \rho_E^{\text{offdiag}} \right] = \mathcal{J}_E(r), \quad (81)$$

which features a fixed Hamiltonian $h_{\text{vac},E} + h_{\text{mat}} + h_{\text{self}}^{(0)}$. In other words, this equation virtually describes a noncollective flavor evolution and it is straightforward to show that

$$\|\delta \rho_E^{\text{offdiag}}(r)\|_F \leq \int_{R_\nu}^r \|\mathcal{J}_E(r')\| dr', \quad (82)$$

where $\|\mathcal{M}\|_F = \sqrt{\text{tr}(\mathcal{M}^\dagger \mathcal{M})}$ is the Frobenius norm of a matrix and $\|\mathcal{J}_E(r')\|$ is the spectral norm. The latter being equal to $|\mu_{12} B_\perp(r')| \cdot \|\rho_E^{(0)}(r')\|$ up to a factor of order unity, we conclude that block-off-diagonal perturbations $\delta \rho_E^{\text{offdiag}}$ grow linearly with distance, not exhibiting exponential growth. As for the block-diagonal part $\delta \rho_E^{\text{diag}}$ of the perturbation, it obeys the same equation (79) as in the $\mu_{12} = 0$ case, when the density matrix is exactly block diagonal at all r . Instabilities are well known to exist here, both in the absence of NSSIs, $g_+ = g_- = 0$ [9], and in their presence, $g_+ = 0, g_- \neq 0$ [34], but they contain no signatures of a nonzero magnetic moment in the linear regime.

We are thus able to conclude that in the absence of a scalar-pseudoscalar NSSI, i.e., within the electroweak theory, a tiny magnetic moment of a Majorana neutrino does not trigger new unstable modes that could result in observable signatures in the neutrino spectra. In order to leave such a signature, the transition magnetic moment should be at least of the order of $1/|B_\perp|L$, where L is the distance covered by the neutrino [see Eq. (82)]; for $L \sim R_\nu \sim 50$ km and $|B_\perp| \sim 10^{12}$ Gauss, this amounts to about $0.5 \times 10^{-15} \mu_B$. In the next section, we will show numerically that this statement also holds true beyond the linear stability regime. Note also that the argument that has led to such a conclusion was based only on the block structure of the Hamiltonian matrix, thus, it can be repeated beyond the single-angle scheme, i.e., for the Hamiltonian (57).

Let us now turn on the block-off-diagonal NSSI, $g_+ \neq 0$. Even in this case, Eq. (79) tells us that the fate of block-diagonal perturbations is determined solely by g_- and provides no signatures of a nonzero μ_{12} . The block-off-diagonal modes follow Eq. (80), which, in general, has to be treated numerically. However, to probe the possibility of unstable modes, it is usually instructive to carry out a Lyapunov stability analysis. For that, first, the source term in the evolution equation (80) is omitted but is replaced by a nontrivial initial perturbation $\delta\rho_E^{\text{offdiag}}(R_\nu)$ on top of a diagonal reference matrix $\rho_E^{(0)}(R_\nu)$ of the form (71). Second, assuming that the mixing angle is virtually zero and (for our toy model) that neutrinos are monochromatic with energy E_0 , we arrive at a constant nonperturbed solution:

$$\begin{aligned} \rho_E^{(0)}(r) &= \rho_E^{(0)}(R_\nu) \equiv \rho^{(0)} \delta(E - E_0), \\ \rho^{(0)} &= \text{diag}(s_{\nu_e}, s_{\nu_x}, s_{\bar{\nu}_e}, s_{\bar{\nu}_x}). \end{aligned} \quad (83)$$

$$\mathbb{L}_A = \begin{pmatrix} \Omega_- + 3\mu(\Delta s_e + \Delta s_x) & 0 & \mu g_+(s_{\nu_e} - s_{\bar{\nu}_x}) & -\mu g_+(s_{\nu_e} - s_{\bar{\nu}_x}) \\ 0 & \Omega_+ + 3\mu(\Delta s_e + \Delta s_x) & -\mu g_+(s_{\nu_x} - s_{\bar{\nu}_e}) & \mu g_+(s_{\nu_x} - s_{\bar{\nu}_e}) \\ -\mu g_+(s_{\nu_x} - s_{\bar{\nu}_e}) & \mu g_+(s_{\nu_x} - s_{\bar{\nu}_e}) & -\Omega_+ - 3\mu(\Delta s_e + \Delta s_x) & 0 \\ \mu g_+(s_{\nu_e} - s_{\bar{\nu}_x}) & -\mu g_+(s_{\nu_e} - s_{\bar{\nu}_x}) & 0 & -\Omega_- - 3\mu(\Delta s_e + \Delta s_x) \end{pmatrix}, \quad (88)$$

$$\mathbb{L}_B = 2G_F\sqrt{2}\text{diag}\left(n_e - \frac{n_n}{2}, -\frac{n_n}{2}, -n_e + \frac{n_n}{2}, \frac{n_n}{2}\right) + 2\mu \text{diag}(\Delta s_e + \Delta s_x, \Delta s_e + 2\Delta s_x, -2\Delta s_e + \Delta s_x, -\Delta s_e - 2\Delta s_x), \quad (89)$$

where $\xi = (\xi_1, \xi_2, \dots, \xi_8)^T$, $\Delta s_{e,x} \equiv s_{\nu_{e,x}} - s_{\bar{\nu}_{e,x}}$, $\Omega_\pm = G_F\sqrt{2}(n_e - n_n) \pm \eta\omega$, $\omega = \Delta m^2/2E_0$ is the vacuum oscillation frequency, and $\eta = \pm 1$ is the mass hierarchy. The diagonal block \mathbb{L}_B has real eigenvalues, while the eigenvalues of a non-Hermitian 4×4 matrix \mathbb{L}_A may be complex if the initial neutrinos possess a flavor imbalance,

Finally, let us assume that inhomogeneities of the matter and neutrino number densities are negligible at the typical growth scale of unstable perturbations. Under these assumptions, we arrive at a linear homogeneous equation with constant coefficients governing the growth of perturbation $\delta\rho_E^{\text{offdiag}}(r) \equiv \delta Q(r)\delta(E - E_0)$:

$$\begin{aligned} i\frac{\partial \delta Q}{\partial r} &= \mathbb{L}(\delta Q), \\ \mathbb{L}(\delta Q) &\equiv \left[h_{\text{vac}, E_0} + h_{\text{mat}} + h_{\text{self}}^{(0)}, \delta Q \right] + \left[\delta h_{\text{self}}^{\text{offdiag}}, \rho^{(0)} \right], \end{aligned} \quad (84)$$

$$\delta h_{\text{self}}^{\text{offdiag}} = \mu g_+(\delta Q^T - \delta Q^c), \quad (85)$$

where $\mu = G_F\sqrt{2}\mathcal{D}(r/R_\nu)n_\nu(r)$ is the neutrino-neutrino coupling strength. Now the question of linear stability reduces to existence of nonreal eigenvalues of a linear map \mathbb{L} . Parametrizing the (block-off-diagonal) perturbation matrix as

$$\delta Q \equiv \begin{pmatrix} 0 & 0 & \xi_5 & \xi_1 \\ 0 & 0 & \xi_2 & \xi_6 \\ \xi_7 & \xi_3 & 0 & 0 \\ \xi_4 & \xi_8 & 0 & 0 \end{pmatrix}, \quad (86)$$

one writes the eigenvalue equation for $\mathbb{L}(\delta Q) = \lambda\delta Q$ in a vectorized form,

$$\mathbb{L}_{\text{vec}}\xi = \lambda\xi, \quad \mathbb{L}_{\text{vec}} \equiv \begin{pmatrix} \mathbb{L}_A & 0 \\ 0 & \mathbb{L}_B \end{pmatrix}, \quad (87)$$

$s_{\nu_{e,x}} \neq s_{\bar{\nu}_{e,x}}, s_{\bar{\nu}_{x,e}}$. Further we will plot the instability rates κ_{max} , i.e., the maximum imaginary parts of the eigenvalues of \mathbb{L}_A , for $s_{\nu_e} = 1$, $s_{\bar{\nu}_e} = \alpha \geq 0$, and $s_{\nu_x} = s_{\bar{\nu}_x} = 0$, changing the neutrino intensity parameter μ and the NSSI coupling g_+ . In fact, for the matter potential $V_{e,n} \equiv G_F\sqrt{2}n_{e,n}$ set to zero, the eigenvalues of \mathbb{L}_A can be found analytically,

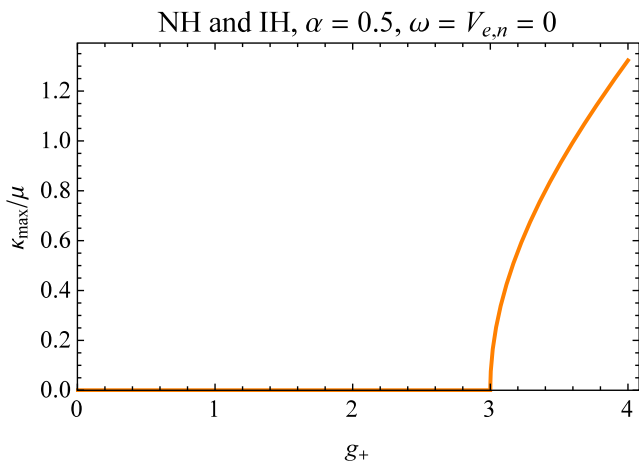


FIG. 1. Growth rates corresponding to a fast unstable mode for a monochromatic neutrino flux, depending on the NSSI coupling g_+ . The plot demonstrates the asymptotic case with both the vacuum oscillation frequency ω and the matter potentials $V_{e,n}$ neglected.

$$\lambda_{1,2,3,4} = \pm \sqrt{\omega^2 + (1 - \alpha)^2 (9 - g_+^2/2) \mu^2 \pm \mu \sqrt{D}},$$

$$D = g_+^4 (1 - \alpha)^4 \mu^2/4 + 4[9(1 - \alpha)^2 + \alpha g_+^2] \omega^2 + 6g_+^2 (1 + \alpha) (1 - \alpha)^2 \eta \omega \mu.$$

From this equation, one observes that for a strong NSSI coupling $|g_+| > 3$, instabilities survive even in the ultradense neutrino gas regime $\omega = V_{e,n} = 0$, their growth rate being $\kappa_{\max} = \sqrt{g_+^2 - 9} \mu |1 - \alpha|$. This corresponds to a so-called *fast* unstable mode (see, e.g., Refs. [14–16]), whose growth rates for $\omega, V_{e,n} \ll \mu$ are of the order of μ . It is well known that there are no such modes in the single-angle scheme with purely electro-weak (V–A) neutrino-neutrino interactions: all instabilities disappear as $\omega \rightarrow 0$ [9]. Moreover, interestingly, the unstable mode we have obtained survives in the absence of antineutrinos ($\alpha = 0$), whereas Standard-Model interactions do not generate instabilities in this case, within the monochromatic setup being discussed. In contrast, scalar-pseudoscalar NSSI, as we see, does generate a fast unstable mode even for monochromatic neutrinos, and its growth rate is plotted in Fig. 1. However, we will not discuss this mode here, since we are more interested in unstable modes present for a small NSSI coupling. These come from an eigenvalue branch with $\lim_{\omega \rightarrow 0} \text{Im} \lambda(\omega) = 0$, thus, these instabilities are *slow*, i.e., suppressed in the $\omega \ll \mu$ regime.

The instability rates for the slow modes are plotted in Figs. 2 and 3 for different neutrino/antineutrino ratios α and both hierarchies. One observes that the presence of

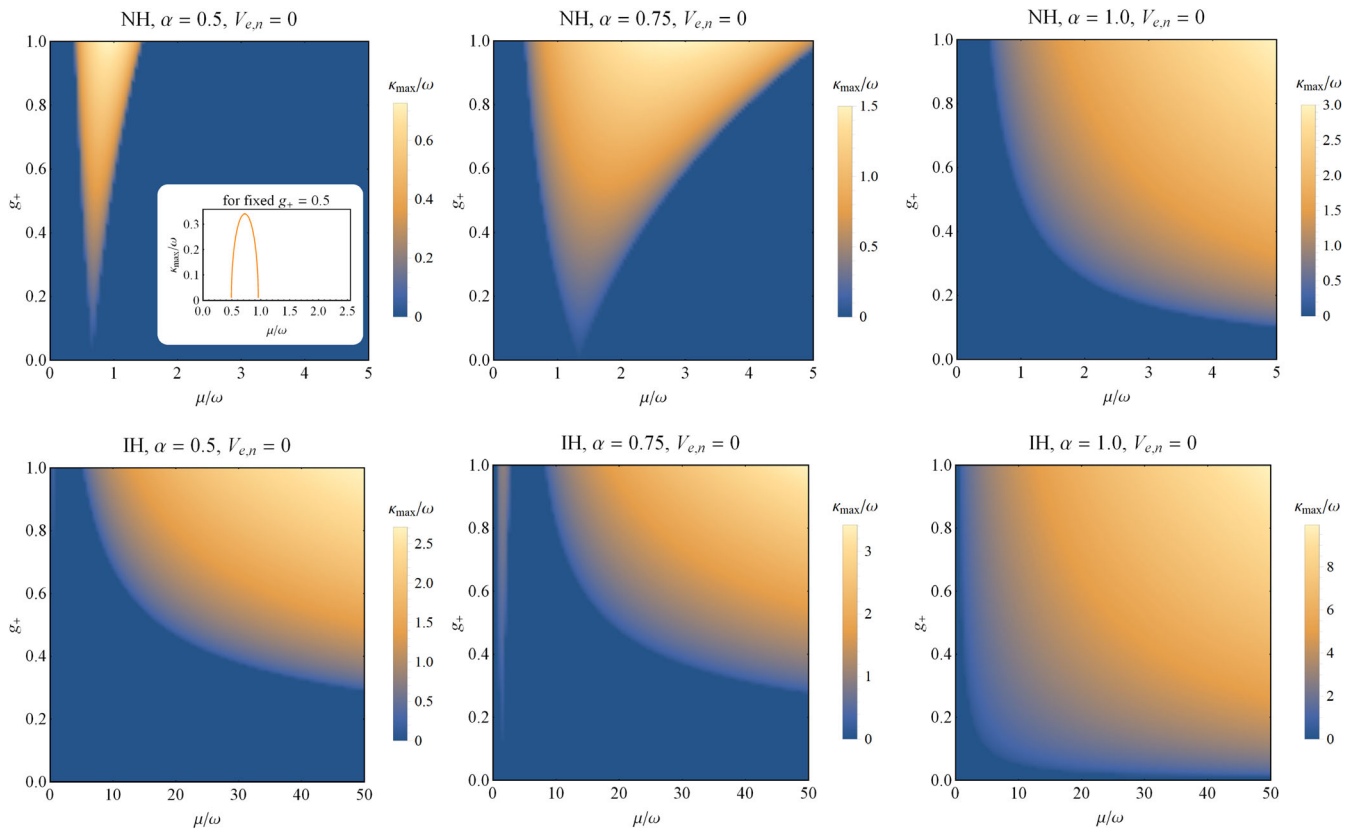


FIG. 2. Instability growth rates for a monochromatic neutrino flux due to the presence of a block-off-diagonal NSSI with parameter g_+ . Inset: instability growth rate as a function of the neutrino number density for a fixed NSSI coupling $g_+ = 0.5$. The background matter density is set to zero in all panels.

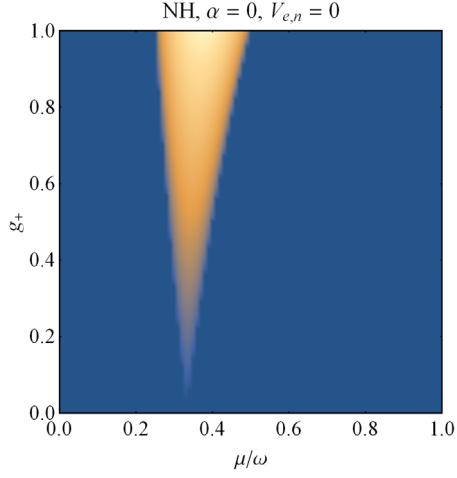


FIG. 3. Instability growth rates for a monochromatic purely electron neutrino flux due to the presence of a block-off-diagonal NSSI with parameter g_+ . The background matter density is set to zero.

antineutrinos considerably enhances the instability region; for normal hierarchy ($\eta = +1$), in fact, the widest instability “sector” in the $(\mu/\omega, g_+)$ plane corresponds to $\alpha = 1$. This sector touches the $g_+ = 0$ line at a resonant neutrino density $\mu = \omega/3|1 - \alpha|$, i.e., for such a density, the studied type of instabilities arises for arbitrarily small g_+ . The $\alpha = 0$ case, corresponding to flavor instabilities of a monochromatic purely ν_e flux, is worth special attention: as we mentioned above, instabilities are absent here in the conventional V–A case, while NSSI triggers them for the normal hierarchy *only* near the resonance $\mu \sim \omega/3$ (Fig. 3). This effect may have implications for the flavor evolution of predominantly electron neutrinos produced during the early neutronization phase of a supernova explosion [41]. In the presence of antineutrinos, instabilities do arise for both mass hierarchies, but the patterns for the inverted one are quite different (see the lower row in Fig. 2), also presenting another, high-neutrino-density instability region. In both cases, as one observes, these *slow* instabilities should grow at typical scales smaller than the vacuum oscillation length, i.e., at several kilometers or even smaller.

Let us now discuss the effect of background matter, i.e., nonzero $V_{e,n}$ potentials, on the stability properties of our system. Interestingly, in the presence of neutrino-antineutrino NSSI coupling, a transformation to a corotating frame in the flavor space does not let one eliminate the MSW term, as it does for $g_{\pm} = 0$ [9]. Namely, a substitution

$$\delta\varrho(r) = \exp\left\{-i \int_{R_v}^r h_{\text{mat}}(r') dr'\right\} \delta\tilde{\varrho}(r) \times \exp\left\{i \int_{R_v}^r h_{\text{mat}}(r') dr'\right\} \quad (90)$$

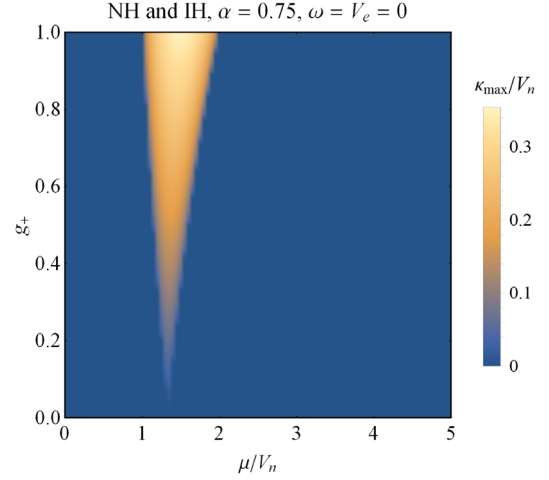


FIG. 4. Instability growth rates for a monochromatic neutrino flux due to the presence of a block-off-diagonal NSSI interaction with parameter g_+ . In contrast to Fig. 2, a neutron background is added with Wolfenstein potential V_n , while the contribution of background electrons V_e and the vacuum oscillation frequency ω are neglected.

into the equation of motion (84) for the instability does not totally “hide” the MSW term into the unitary transformation because of the matrix structure of the block-off-diagonal NSSI interaction (85). Note that both the electroweak ($g_{\pm} = 0$) interaction Hamiltonian and the Hamiltonian (73) from Ref. [6] feature a combination of the form $\rho - \rho^{cT}$ instead of a scalar-pseudoscalar $\rho^T - \rho^c$ in Eq. (85), which lets one eliminate the MSW term by a unitary transformation to a corotating frame. Physically, this results in the fact that in the presence of NSSI, background matter modifies the instability rates; in particular, one observes that even when $\omega = 0$ and $V_{e,n} \neq 0$, there are “intermediate” (neither fast, nor slow) unstable modes whose rates κ are proportional to $V_{e,n}$. Indeed, in a typical supernova situation, $\mu \gtrsim V_{e,n} \gg \omega$ near the neutrino sphere, thus, these should be considerably faster than the *slow* ones. Correspondingly, the two possibly nonreal eigenvalues in the $\omega = 0$ case read

$$\lambda_{1,2} = \pm \sqrt{(V_e - V_n + 3(1 - \alpha)\mu)^2 - g_+^2(1 - \alpha)^2\mu^2}. \quad (91)$$

In particular, from this expression, it follows that for a small NSSI coupling, instabilities take place in a narrow resonance region around $\mu = (V_n - V_e)/3(1 - \alpha)$. In Fig. 4, we demonstrate their growth rates for an idealized situation $\omega = V_e = 0$; the pattern looks quite similar to Fig. 2, but now the rates are measured in V_n instead of ω , i.e., they are higher.

As we see, the block-off-diagonal NSSI coming from the scalar and pseudoscalar terms in the Lagrangian may lead to fast, slow, and intermediate instabilities that remain hidden in the absence of neutrino magnetic moment (or

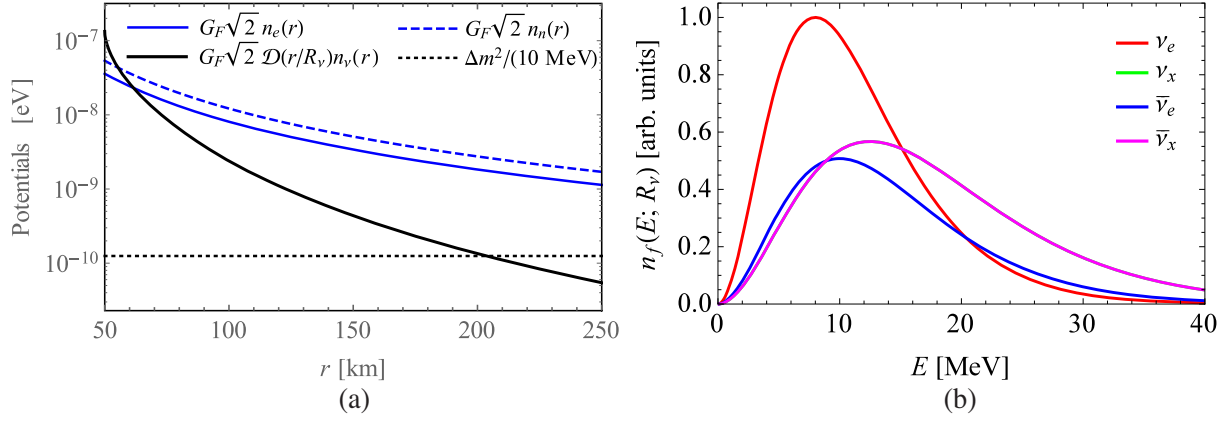


FIG. 5. (a) Comparison of matter (neutron, electron) potentials, the neutrino self-coupling, and the energy scale of vacuum oscillations for a star with luminosity $L = 10^{55} \text{ sec}^{-1}$. (b) The initial flavor/energy spectra at the neutrino sphere $r = R_\nu$ used in the simulations.

external magnetic field). Within the purely electroweak interaction model, these modes are also absent.

IV. NUMERICAL SIMULATION

Lyapunov stability analysis carried out in the previous section provides an insight into the effect of a small magnetic moment of a Majorana neutrino on collective oscillations, however, it is based on a number of artificial assumptions limiting the status of its conclusions. Moreover, in reality, one is interested in non-negligible NSSI/magnetic moment signatures in the observable neutrino energy spectra, which is beyond the regime of linear perturbations on top of a stationary nonperturbed solution. To explore the issue and estimate the sensitivities of the neutrino spectra to the magnetic moment, in the present section we carry out a numerical analysis of collective oscillations with the block-off-diagonal NSSI within the single-angle scheme.

For our simulation, we work with two neutrino flavors with $\Delta m^2 = 2.4 \times 10^{-3} \text{ eV}^2$ and $\theta = 9^\circ$ [36]. The supernova setup is analogous to the one used, e.g., in [6]. Namely, a neutrino is leaving the neutrino sphere with the radius $R_\nu = 50 \text{ km}$ radially in the equatorial plane, so that the transversal component of the magnetic field decays as an inverse power law with r ,

$$B_\perp(r) = B_{\text{surf}} \left(\frac{R_\nu}{r} \right)^2, \quad B_{\text{surf}} = 10^{12} \text{ Gauss.} \quad (92)$$

The neutrino density profile and the geometric factor together form an effective neutrino-neutrino coupling,

$$\begin{aligned} \mu(r) &\equiv G_F \sqrt{2} n_\nu(r) \mathcal{D}(r/R_\nu) \\ &= G_F \sqrt{2} \times \frac{L}{2\pi R_\nu^2} \times \frac{1}{2} \left(1 - \sqrt{1 - (R_\nu/r)^2} \right)^2, \end{aligned} \quad (93)$$

where L is the neutrino luminosity parameter, namely, the number of emitted neutrinos per second (we follow the convention of Ref. [9] dividing it by $2\pi R_\nu^2$). By default we take $L = 10^{55} \text{ sec}^{-1}$ corresponding to the total radiation power $L \times 10 \text{ MeV} \sim 1.5 \times 10^{50} \text{ erg/sec}$. The electron density is chosen following the single-angle simulations in Ref. [6], while we also add neutrons with the density $n_n = 1.5n_e$. The potentials $V_{e,n}(r) = G_F \sqrt{2} n_{e,n}(r)$ and the above neutrino-neutrino coupling are shown in Fig. 5(a), together with the energy scale $\omega = \Delta m^2 / (2 \times 10 \text{ MeV})$ of vacuum oscillations. At the neutrino sphere, the flavor density matrix is diagonal [see Eq. (71)], with the energy spectra taken from a simulation [42] [see Fig. 5(b)]; these spectra are nothing but Fermi distributions for the three different decoupling temperatures of ν_e , $\bar{\nu}_e$, and $\nu_x/\bar{\nu}_x$. Upon evolution (65), the flavor/energy spectra are extracted from the density matrix with the help of a flavor/helicity projector \mathcal{P}_f :

$$\begin{aligned} n_f(E; r) &= \text{tr}(\rho_E(r) \mathcal{P}_f) = (\rho_E(r))_{f,f}, \\ f &= e, x, \bar{e}, \bar{x} (e-, x-, e+, x+). \end{aligned} \quad (94)$$

We study the region $R_\nu \leq r \lesssim 250 \text{ km}$ far from the MSW resonance ($V_{e,n} \gg \Delta m^2 \cos 2\theta / 2E$), in which the oscillations are mainly driven by collective effects. Moreover, in reality, the neutrino self-coupling falls off quite rapidly, so that the oscillations virtually freeze around $r = 200\text{--}250 \text{ km}$ producing well-defined “final” neutrino spectra on exit from the region. It is these spectra produced by nonlinear, collective effects that we are interested in within our analysis of NSSI-induced flavor instabilities.

Let us first discuss the flavor evolution without (pseudo)scalar NSSIs, i.e., within the (minimally extended)

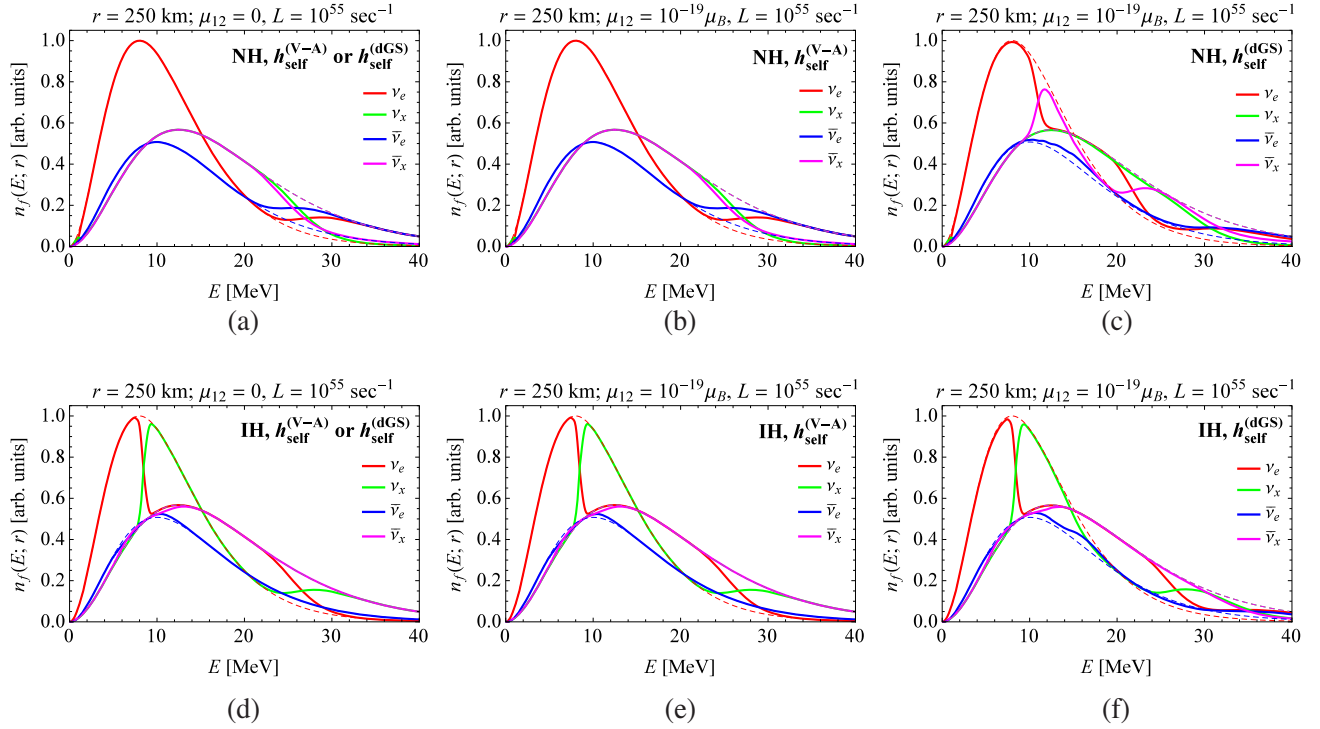


FIG. 6. The effect of the neutrino magnetic moment on the neutrino spectra without (pseudo)scalar NSSI for $L = 10^{55} \text{ sec}^{-1}$. The upper and the lower rows correspond to the normal and the inverted hierarchies, respectively. The first column [(a) and (d)] shows the case $\mu_{12} = 0$, the second [(b) and (e)] the $\mu_{12} \neq 0$ case with self-interaction Hamiltonian (69), and the last one [(c) and (f)] also to $\mu_{12} \neq 0$, but based on the Hamiltonian (73) from Ref. [6]. Dashed lines sketch the initial spectra at the neutrino sphere [Fig. 5(b)]. In the $\mu_{12} = 0$ case, the two Hamiltonians produce the same result. Visual identity of [(a) and (c)] and [(b) and (d)] plots, respectively, holds up to at least $|\mu_{12}| \sim 10^{-15} \mu_B$.

Standard Model, comparing the effect of the self-interaction Hamiltonian (69) derived by us and that of the Hamiltonian (73) claimed in Ref. [6]. As mentioned in Sec. II, these two Hamiltonians lead to identical flavor evolutions in the $\mu_{12} = 0$ case. Figure 6 shows the results of the simulation for $\mu_{12} \neq 0$, in the cases where the effect is visually noticeable. It turns out that with our Hamiltonian the final spectra are virtually insensitive to the neutrino magnetic moment up to at least $|\mu_{12}| \sim 10^{-15} \mu_B$, while the evolution with self-interaction (73) contains considerable magnetic moment signatures already for $\mu_{12} = 10^{-19} \mu_B$, especially in the normal hierarchy (the latter was, in fact, stated in [6]). For a luminosity $L = 10^{54} \text{ sec}^{-1}$ 1 order of magnitude lower than that in Fig. 6, the magnetic moment signatures virtually disappear, obviously because the instabilities causing them get suppressed. Note that the low sensitivity of the evolution equations (65) to the magnetic moment of a Majorana neutrino agrees with the linear stability analysis in Sec. III, so that we have to conclude that within the Standard Model without NSSIs, the effect of a small magnetic moment should be quite hard to observe. This has also been noted in our previous analysis [26]; the case of a large neutrino magnetic moment has been recently studied in [27], including the angular neutrino

distributions, and the analysis demonstrates that for a smaller magnetic moment/weaker magnetic field, their signatures are suppressed. Regarding the Hamiltonian (73) that was claimed to hold within the Standard Model in Ref. [6], we have to consider it a nonstandard neutrino self-interaction instead, which leads to a pronounced effect of the neutrino transition magnetic moment.

Now let us switch to the main issue of the present paper, namely, to the effect of nontrivial scalar/pseudoscalar NSSIs on the collective neutrino flavor evolution. Namely, for the same luminosity $L = 10^{55} \text{ sec}^{-1}$, we set the block-diagonal NSSI coupling g_- to zero (as mentioned earlier, this coupling has been analyzed in other papers [34]), keeping only the block-off-diagonal term with the g_+ coupling, and analyze the effect of this small NSSI for a small transition magnetic moment $\mu_{12} = 10^{-19} \mu_B$. Again, when the magnetic moment is zero, the density matrix becomes block diagonal and the g_+ coupling produces zero effect on the oscillations. For a nonzero magnetic moment, in contrast, nonstandard interactions radically change the neutrino spectra, see Fig. 7.

Indeed, neutrino-antineutrino instability caused by the block-off-diagonal NSSI and triggered by the μB interaction shows up in both hierarchies provided that the NSSI

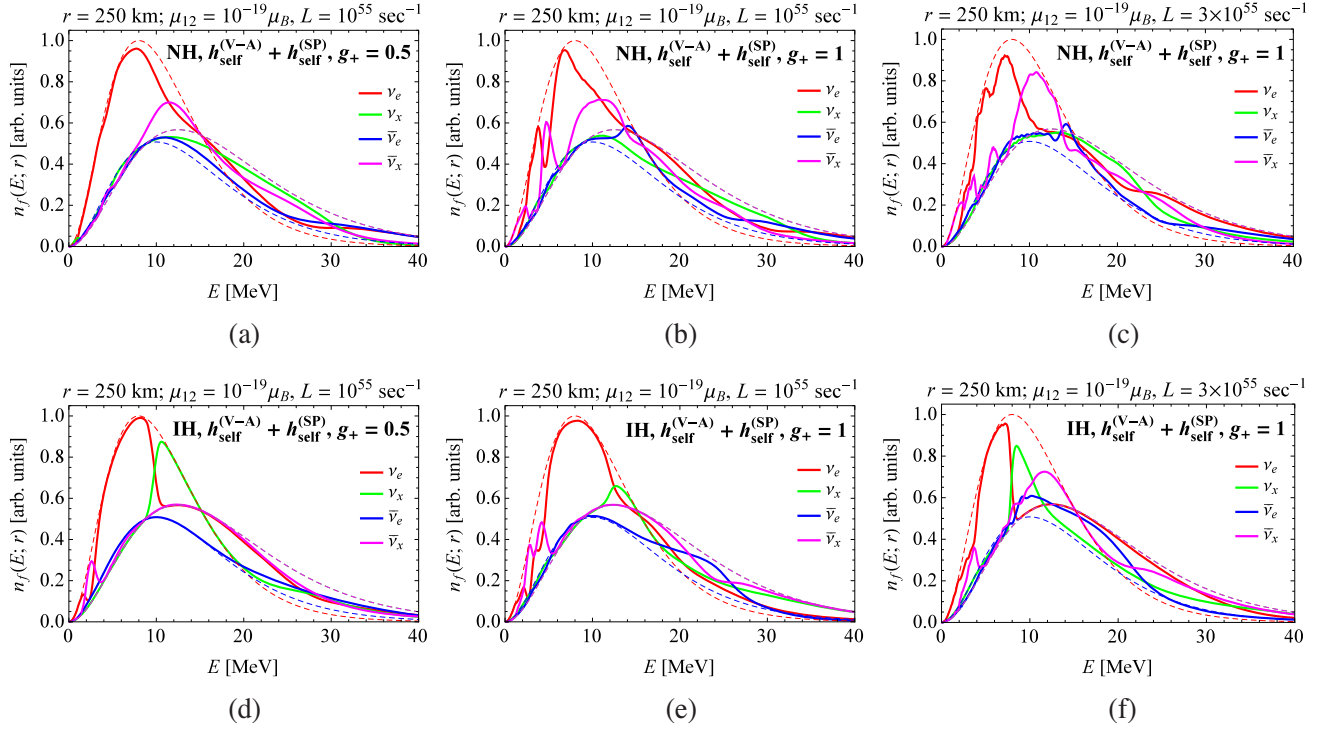


FIG. 7. The effect of the block-off-diagonal NSSI on the neutrino spectra for the neutrino magnetic moment $\mu_{12} = 10^{-19} \mu_B$ and different NSSI couplings g_+ and luminosities L . The upper and the lower rows correspond to the normal and the inverted hierarchies, respectively. The first [(a) and (d)] and the second [(b) and (e)] columns demonstrate the cases with luminosity $L = 10^{55} \text{ sec}^{-1}$ and different NSSI couplings; the last column [(c) and (f)] shows the results for $L = 3 \times 10^{55} \text{ sec}^{-1}$. Dashed lines sketch the initial spectra at the neutrino sphere [Fig. 5(b)].

coupling is not too small, $|g_+| \gtrsim 0.3$, and rapidly leads to a complicated, if not a chaotic pattern. This is clearly manifested in the wiggly patterns in Fig. 7 resulting from probability exchange between ν_e and $\bar{\nu}_x$ flavors. For large g_+ couplings, this exchange even results in a $\nu_e - \bar{\nu}_x$ spectral split, which replaces the $\nu_e - \nu_x$ split in the inverted hierarchy case. In fact, animations of the flavor evolution we made also reveal that $g_+ \neq 0$ flavor evolution

starts from rapid synchronized oscillations of the spectra with typical lengths of 10–100 m (in contrast to the no-NSSI case, where the oscillation lengths are of the order of 10 km), which, in principle, agrees with our conclusions on the fast/intermediate instabilities in Sec. III.

The effects do not drastically depend on the magnetic moment, since it acts just as a seed for an exponentially growing instability; deformation of the spectra can be

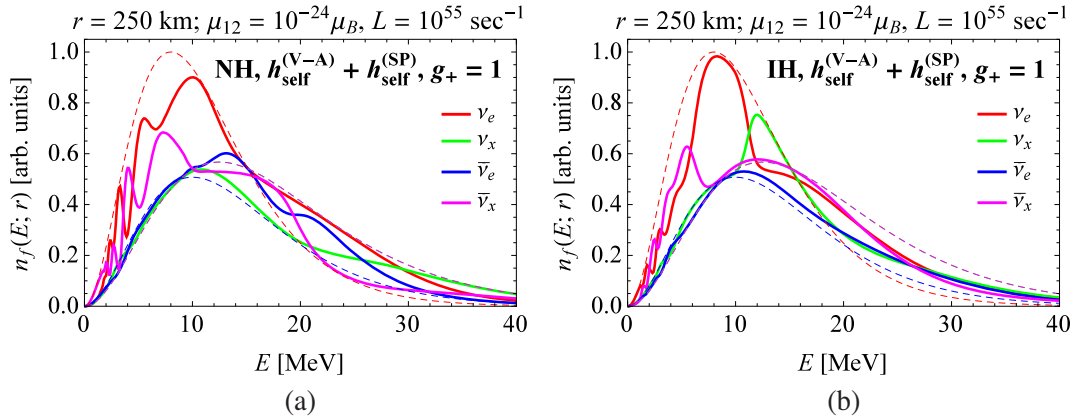


FIG. 8. Impact of scalar-pseudoscalar NSSI with $g_+ = 1$ on the neutrino flavor evolution for $L = 10^{55} \text{ sec}^{-1}$ and a very small magnetic moment $\mu_{12} = 10^{-24} \mu_B$ for the two mass hierarchies.

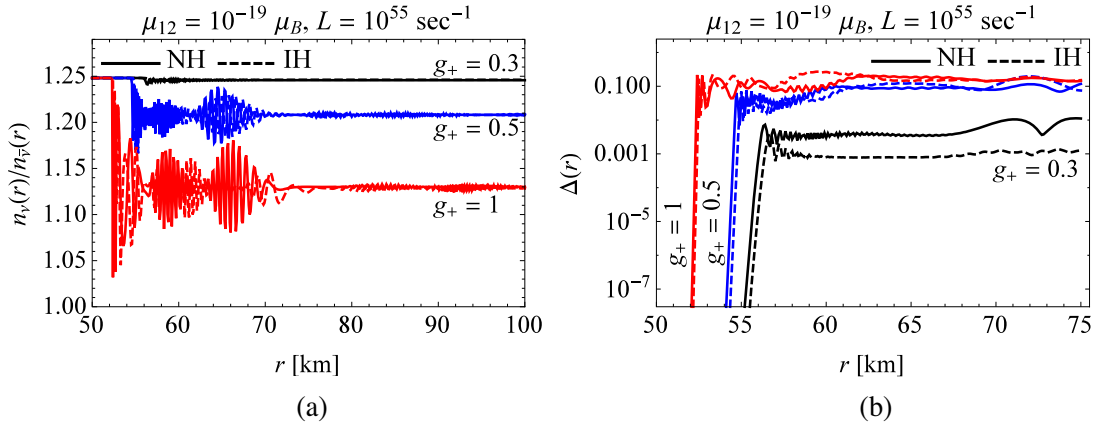


FIG. 9. Impact of scalar-pseudoscalar NSSI on the neutrino flavor evolution for $L = 10^{55} \text{ sec}^{-1}$ and $\mu_{12} = 10^{-19} \mu_B$ for different NSSI couplings and mass hierarchies: (a) evolution of neutrino-to-antineutrino number ratio; (b) evolution of spectral residuals (95).

observed even for $\mu_{12} \sim 10^{-24} \mu_B$ (see Fig. 8).¹ On the other hand, the rates of instabilities resulting in nontrivial NSSI signatures strongly depend on the degree of non-linearity of the equations, i.e., on the luminosity, and these signatures are virtually absent for $L = 10^{54} \text{ sec}^{-1}$.

Let us now take a closer look at the development of NSSI-induced instabilities for $L = 10^{55} \text{ sec}^{-1}$ and address the issue of their potential observability. First of all, a natural parameter controlling these neutrino-antineutrino instabilities is the ratio of the total neutrino and antineutrino numbers $n_\nu(r)/n_{\bar{\nu}}(r)$ obtained after integration over the whole energy spectrum. This ratio is conserved in the absence of magnetic moment μ_{12} ; however, as we saw above, it is also conserved to a high accuracy even when μ_{12} is nonzero, in both noncollective oscillations and collective oscillations without NSSIs, neither of which contain neutrino-antineutrino instabilities. Interestingly, Fig. 9(a) demonstrates that when NSSIs come into play, the total neutrino and antineutrino numbers rapidly reach an equilibrium plateau. This phenomenon resembles a sort of equilibration discussed in Ref. [27], but for a value of $\mu_{12}B$ that is many orders of magnitude smaller. The equilibrium neutrino-antineutrino ratio is then conserved up to the neutrino detector, so that antineutrino excess could, in

principle, serve as a signature of NSSIs mixing neutrinos with antineutrinos, such as scalar and pseudoscalar interactions.

Figure 9(a) also reveals a *fast* character of the instability, as opposed to *slow* instabilities with growth scales of the order of 10 km. To quantify this instability and the resulting impact of the neutrino spectra, we introduce a spectral residual as the relative integral deviation of the neutrino flavor spectra from the no-magnetic-moment case, in which the effect of NSSIs is absent

$$\Delta(r) = \frac{\sum_f \int |n_f(E; r) - n_f^{(0)}(E; r)| dE}{\sum_f \int n_f^{(0)}(E; r) dE}, \quad (95)$$

where $n_f^{(0)}(E; r)$ correspond to the flavor-energy spectra for $\mu_{12} = 0$ and the summation is performed over both neutrino and antineutrino flavors. Now, Fig. 9(b) clearly demonstrates a drastic difference between the evolutions of neutrino spectra for $g_+ \leq 0.3$ and $g_+ \gtrsim 0.5$: in the latter case, the residuals $\Delta(r)$ rapidly saturate to quite observable values of the order of 10^{-1} and keep this level during further evolution. Note that the level $\Delta \sim 0.01$ – 0.1 corresponds, in fact, to quite a large spectral distortion, such as those shown in Fig. 7. Finally, the spectral residuals at the final point $r = 250 \text{ km}$ are shown in Fig. 10 versus the luminosity L and the NSSI coupling g_+ . One observes that at least for $L \leq 10^{56} \text{ sec}^{-1}$, one can probe the NSSI coupling with the sensitivity around 0.25–0.4 in both mass hierarchies. It is important, however, that this order of sensitivity can be achieved for extremely small values of the neutrino transition magnetic moments, comparable with the figures predicted within the minimally extended Standard Model with the standard, V–A structure of weak interactions [23,43].

¹Interestingly, such a small value of the magnetic moment does not lead to large roundoff errors in the numerical integration, roughly speaking, coming from addition of “large” and “small” matrices in expressions of the form $\rho(r + \Delta r) \approx \rho(r) - i\Delta r[h(r), \rho(r)]$. The reason is that during the early stages of the evolution ρ is approximately block diagonal, so adding a small but block-off-diagonal matrix $-i[h_{\text{AMM}}, \rho]$ to it does not round the latter one down to zero: the large blocks are not added to small blocks of the density matrix. During the later stages, it is mainly the self-interaction and not the tiny magnetic moment that drives the evolution of the density matrix.

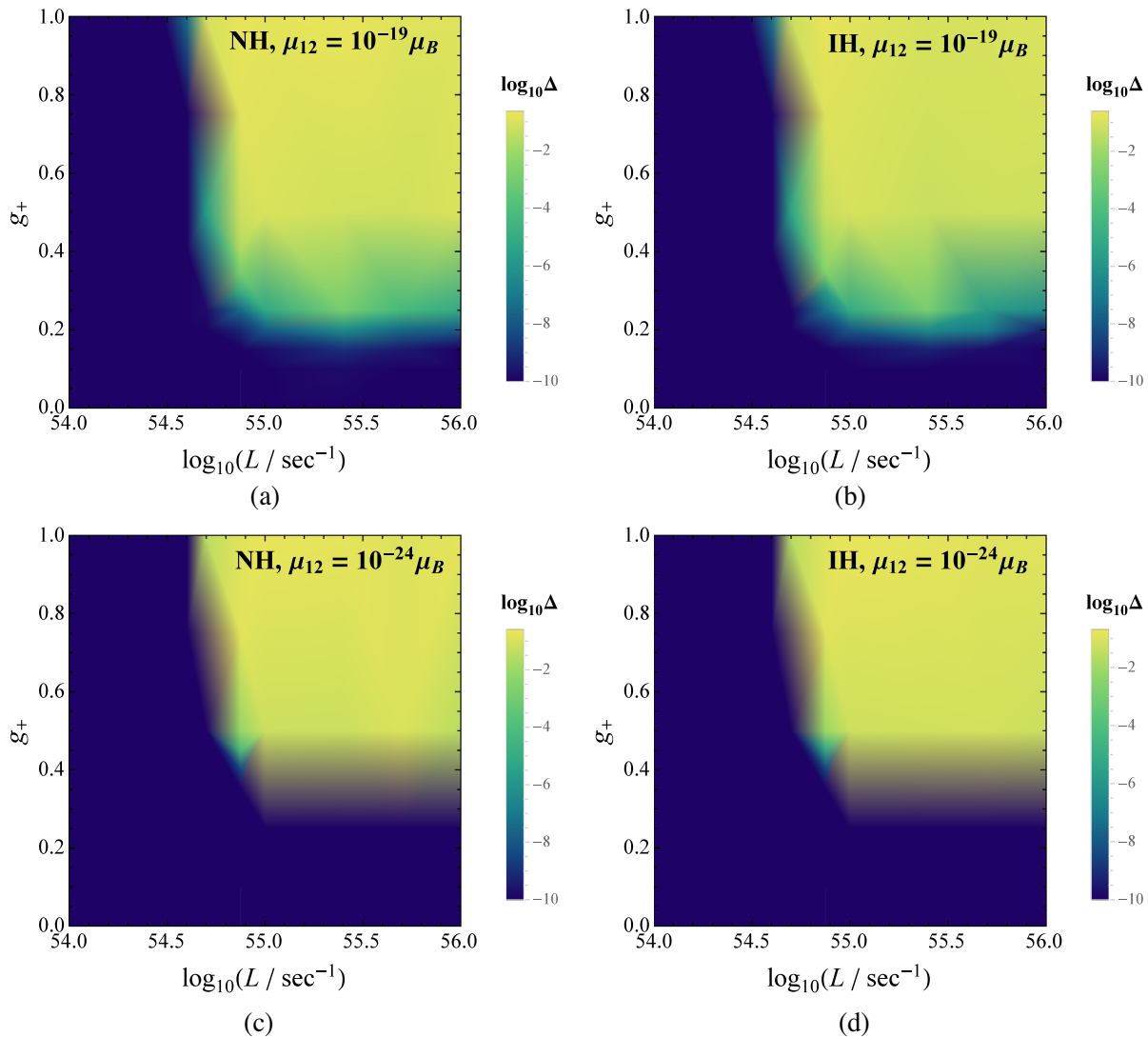


FIG. 10. Sensitivity of collective neutrino oscillations to the NSSI coupling g_+ in terms of the spectral residual Δ (250 km), depending on the coupling g_+ and the luminosity L . The magnetic moment is set to $\mu_{12} = 10^{-19}\mu_B$ and $10^{-24}\mu_B$ in the two upper and lower panels, respectively.

V. DISCUSSION

The analysis given in the above sections has led us to a number of interesting conclusions regarding the effect of nonstandard, scalar and/or pseudoscalar four-fermion neutrino interactions on the collective oscillations taking place during a supernova explosion. First, it turned out that such NSSIs include the terms that mix neutrinos and antineutrinos, and these are able to open up a new channel of fast neutrino-antineutrino instabilities considerably deforming the neutrino flavor-energy spectra. In fact, these spectral features, including nonstandard splits and chaotic-looking patterns, need a seed to develop; however, a minuscule transition neutrino magnetic moment $\mu_{12} \sim 10^{-24}\mu_B$ proves to be enough to trigger the effect via neutrino-antineutrino (helicity flip) transitions in the stellar magnetic field. Note that such a transition magnetic moment could be

generated even at the one-loop level of the Standard Model, in which a Glashow-Iliopoulos-Maiani cancellation takes place [23,43].

Second, the discussed type of $\nu - \bar{\nu}$ instability is also quite nonstandard in that the electron/neutron background nontrivially affects the instability rates even for monochromatic neutrinos and in that these instabilities survive in the absence of antineutrinos (see Sec. III devoted to linear stability analysis). From this analysis we also observed that, quite as usual, a neutrino-antineutrino ratio close to unity favors the development of instabilities.

Third, the sensitivity of (anti)neutrino spectra to the NSSI coupling stays at the level of $g_+ \sim 0.3$ for neutrino luminosities $L \gtrsim 10^{55} \text{ sec}^{-1}$, notably, virtually regardless of the (nonzero) value of the magnetic moment. Note that the spectral residual Δ (250 km) chosen by us to quantify the NSSI signatures in the neutrino spectra [see Eq. (95)]

can change outside the $r = 250$ km sphere, where collective oscillations are not important, while other effects, such as the MSW effect in a turbulent medium, may come into play [44]. Importantly, however, there is another natural measure of scalar/pseudoscalar NSSI signatures in question, which does not change under (conventional) non-collective oscillations: the neutrino-antineutrino ratio $n_\nu/n_{\bar{\nu}}$. Both this ratio for neutrinos of a given energy E and the one integrated over the whole energy spectrum are almost conserved in noncollective oscillations (the magnetic moment has a negligible effect once the collective oscillations are over), thus, the neutrino-antineutrino ratio (see Fig. 9) should bring the information on the NSSI in the innermost supernova layers to the neutrino detector. Moreover, even though in the present paper we have discussed the NSSI effect on collective oscillations within a simplified picture not including angular degrees of freedom, it is highly likely that the neutrino-antineutrino ratio should depend on the “latitude,” i.e., on the angle between the directions to the stellar magnetic pole and the observer. Therefore, helicity-flipping scalar/pseudoscalar NSSIs could manifest themselves in a periodic variation of the neutrino-antineutrino flux ratio from an explosion of a (rotating) supernova.

Finally, from our analysis, both numerical and analytical, it inevitably turns out that within the framework with a pure V–A interaction, the effective neutrino oscillation Hamiltonian takes the form derived in Ref. [24], which is unable to exponentially catalyze the growth of coherent neutrino-antineutrino mixing initially introduced via the transition magnetic moment. Note that the linear stability analysis in Sec. III that led to this conclusion was not a Lyapunov stability analysis of a necessarily stationary solution, so it does not rely upon a “qualitatively right” assumption of the vanishing vacuum mixing angle. As a result, within the Standard Model extended with nonzero Majorana neutrino masses, the effect of a small nonzero magnetic moment is very unlikely to be observable.

A couple of words should also be said on what was left beyond the present analysis. First of all, Dirac neutrinos should probably have very similar block-off-diagonal terms in the interaction Hamiltonian, if one introduces scalar and/or pseudoscalar terms into the Lagrangian, while in this case these blocks will describe superpositions of active, left-handed neutrinos with “sterile,” right-handed neutrinos rather than neutrino-antineutrino mixing. In the absence of NSSIs, these blocks virtually vanish, so nothing is able to catalyze the helicity-mixing effect introduced by a small magnetic moment, analogously to the Majorana case [26]. Next, we have tested Majorana neutrinos with scalar/pseudoscalar interactions for instabilities initiated by the so-called induced magnetic moment [45], which physically is a helicity-dependent Wolfenstein potential in a magnetized medium, and found no new instabilities. Among other possible reasons, this is definitely related to the fact that at

least for a nonmoving background medium, the induced magnetic moment term in the Hamiltonian does not flip the neutrino helicity. Last but not least, Fig. 9 tells us that (pseudo)scalar NSSIs almost immediately affect the flavor content of the neutrino fluxes, and it seems interesting to analyze whether these fast flavor transformations are able to modify the overall properties of a supernova explosion, possibly leading to conclusions similar to those of Ref. [35]. However, this, as well as other issues regarding the effect of scalar and pseudoscalar nonstandard neutrino self-interactions on the evolution of dense neutrino fluxes require further study beyond the present paper.

ACKNOWLEDGMENTS

The authors are grateful to Maxim Dvornikov and Alexander Grigoriev for fruitful discussions. O. K. would like to give special thanks to Sergei Gladchenko for his attention to the manuscript and for checking a lot of expressions in the preprint after it was published. The research has been carried out using the equipment of the shared research facilities of HPC computing resources at Lomonosov Moscow State University [46]. O. K. would also like to acknowledge kind support with the computational resources from Skolkovo Institute of Science and Technology.

APPENDIX A: BILINEAR EXPRESSIONS FOR MAJORANA NEUTRINOS

We list here the notations and relations for Majorana spinors in the ultrarelativistic regime, which are used to derive the effective Hamiltonian for collective oscillations in Sec. II. We work in the spinor representation, with Dirac matrices

$$\begin{aligned} \gamma^0 &= \begin{pmatrix} 0 & 1 \\ 1 & 0 \end{pmatrix}, & \gamma_5 &= i\gamma^0\gamma^1\gamma^2\gamma^3 = \begin{pmatrix} -1 & 0 \\ 0 & 1 \end{pmatrix}, \\ \boldsymbol{\Sigma} &= \begin{pmatrix} \boldsymbol{\sigma} & 0 \\ 0 & \boldsymbol{\sigma} \end{pmatrix}, \end{aligned} \quad (\text{A1})$$

$$\boldsymbol{\alpha} = \gamma_5 \boldsymbol{\Sigma} = \begin{pmatrix} -\boldsymbol{\sigma} & 0 \\ 0 & \boldsymbol{\sigma} \end{pmatrix}, \quad \boldsymbol{\gamma} = \gamma^0 \boldsymbol{\alpha} = \begin{pmatrix} 0 & \boldsymbol{\sigma} \\ -\boldsymbol{\sigma} & 0 \end{pmatrix}, \quad (\text{A2})$$

$\boldsymbol{\sigma}$ being the Pauli matrices; the commutator of the gamma matrices $\sigma^{\mu\nu} \equiv \frac{i}{2}[\gamma^\mu, \gamma^\nu]$ has components $\sigma^{0i} = i\alpha^i$ and $\sigma^{ij} = \epsilon_{ijk}\Sigma^k$. In this representation, the ultrarelativistic polarization bispinors $u_\alpha(\mathbf{p})$ entering the neutrino field operator (14) become chiral, taking the form

$$\begin{aligned} u_+(\mathbf{p}) &= \begin{pmatrix} 0 \\ \chi_+(\mathbf{p}) \end{pmatrix}, & u_-(\mathbf{p}) &= \begin{pmatrix} \chi_-(\mathbf{p}) \\ 0 \end{pmatrix}, \\ u_\alpha^c(\mathbf{p}) &= u_{-\alpha}(\mathbf{p}), \end{aligned} \quad (\text{A3})$$

where the two-component helicity eigenvectors are defined in the standard way:

$$(\boldsymbol{\sigma} \cdot \mathbf{p})\chi_\alpha(\mathbf{p}) = \alpha|\mathbf{p}|\chi_\alpha(\mathbf{p}), \quad \alpha = \pm 1, \quad (\text{A4})$$

$$\chi_\alpha^\dagger(\mathbf{p})\chi_\beta(\mathbf{p}) = \delta_{\alpha\beta}, \quad -i\alpha\sigma_2\chi_\alpha^*(\mathbf{p}) = \chi_{-\alpha}(\mathbf{p}). \quad (\text{A5})$$

Now a straightforward matrix-vector multiplication, together with the chirality properties of the polarization bispinors, yield a set of bilinear expressions:

$$\bar{u}_\alpha(\mathbf{p})u_\beta(\mathbf{p}) = \bar{u}_\alpha(\mathbf{p})\gamma_5 u_\beta(\mathbf{p}) = 0, \quad (\text{A6})$$

$$\bar{u}_\alpha(\mathbf{p})\gamma^\mu u_\beta(\mathbf{p}) = \delta_{\alpha\beta}(1, \hat{\mathbf{p}}), \quad (\text{A7})$$

$$\bar{u}_\alpha(\mathbf{p})\gamma^\mu\gamma_5 u_\beta(\mathbf{p}) = \alpha\delta_{\alpha\beta}(1, \hat{\mathbf{p}}), \quad (\text{A8})$$

$$\bar{u}_\alpha(\mathbf{p})\gamma_L^\mu u_\beta(\mathbf{p}) = \delta_{\alpha,-}\delta_{\beta,-}(1, \hat{\mathbf{p}}), \quad (\text{A9})$$

$$\bar{u}_\alpha(\mathbf{p})\boldsymbol{\Sigma}u_\beta(\mathbf{p}) = \sqrt{2}\delta_{\alpha,-\beta}\boldsymbol{\zeta}_\beta(\mathbf{p}), \quad (\text{A10})$$

$$\bar{u}_\alpha(\mathbf{p})\boldsymbol{\alpha}u_\beta(\mathbf{p}) = \sqrt{2}\beta\delta_{\alpha,-\beta}\boldsymbol{\zeta}_\beta(\mathbf{p}), \quad (\text{A11})$$

where $\bar{u}_\alpha(\mathbf{p}) \equiv u_\alpha^\dagger(\mathbf{p})\gamma^0$ is a Dirac conjugate, $\hat{\mathbf{p}} \equiv \mathbf{p}/|\mathbf{p}|$, and a complex 3-vector $\boldsymbol{\zeta}_\beta(\mathbf{p})$ is defined as

$$\boldsymbol{\zeta}_\beta(\mathbf{p}) = \frac{1}{\sqrt{2}}\chi_{-\beta}^\dagger(\mathbf{p})\boldsymbol{\sigma}\chi_\beta(\mathbf{p}). \quad (\text{A12})$$

While a couple of properties of this vector follow directly from the above definitions,

$$\mathbf{p} \cdot \boldsymbol{\zeta}_\beta(\mathbf{p}) = 0, \quad (\text{A13})$$

$$|\mathbf{B} \cdot \boldsymbol{\zeta}_\beta(\mathbf{p})| = \frac{1}{\sqrt{2}}|\mathbf{B} \times \hat{\mathbf{p}}|, \quad (\text{A14})$$

$$\boldsymbol{\zeta}_\beta^*(\mathbf{p}) = \boldsymbol{\zeta}_{-\beta}(\mathbf{p}), \quad (\text{A15})$$

$$\boldsymbol{\zeta}_\beta^*(\mathbf{p}) \cdot \boldsymbol{\zeta}_\beta(\mathbf{p}) = 1, \quad (\text{A16})$$

others depend on the $U(1)$ phase $\phi(\mathbf{p})$ in the definition of the two-component helicity eigenstates. Fixing it as

$$\begin{aligned} \chi_+(\mathbf{p}) &= e^{i\phi(\mathbf{p})/2} \begin{pmatrix} \cos \frac{\vartheta}{2} e^{-i\varphi/2} \\ \sin \frac{\vartheta}{2} e^{i\varphi/2} \end{pmatrix}, \\ \chi_-(\mathbf{p}) &= e^{-i\phi(\mathbf{p})/2} \begin{pmatrix} -\sin \frac{\vartheta}{2} e^{-i\varphi/2} \\ \cos \frac{\vartheta}{2} e^{i\varphi/2} \end{pmatrix} \end{aligned} \quad (\text{A17})$$

for the momentum vector $\mathbf{p} = |\mathbf{p}|(\sin \vartheta \cos \varphi, \sin \vartheta \sin \varphi, \cos \vartheta)$ leads to an explicit expression for the $\boldsymbol{\zeta}$ vectors:

$$\begin{aligned} \boldsymbol{\zeta}_\pm(\mathbf{p}) &= \frac{e^{\pm i\phi(\mathbf{p})}}{\sqrt{2}} (\cos \vartheta \cos \varphi \mp i \sin \varphi, \\ &\quad \cos \vartheta \sin \varphi \pm i \cos \varphi, -\sin \vartheta). \end{aligned} \quad (\text{A18})$$

Now one can explicitly evaluate a scalar product entering the effective Hamiltonian (see Sec. II),

$$\boldsymbol{\zeta}_\pm(\mathbf{p}) \cdot \boldsymbol{\zeta}_\pm(\mathbf{q}) = e^{\pm i\Gamma(\hat{\mathbf{p}}, \hat{\mathbf{q}})} \frac{1 - \hat{\mathbf{p}} \cdot \hat{\mathbf{q}}}{2}, \quad (\text{A19})$$

where $\Gamma(\hat{\mathbf{p}}, \hat{\mathbf{q}})$ is another $U(1)$ phase. Even though this phase obviously contains an additive term $\phi(\mathbf{p}) + \phi(\mathbf{q})$, it is easy to see that the Γ phase cannot be eliminated completely by a gauge transformation of $\phi(\mathbf{p})$.

APPENDIX B: AN ANALOG OF THE WICK'S THEOREM

While the original Wick's theorem relates the vacuum expectation value of a product of field operators to a set of pairwise contractions, the *approximate* theorem we have used in Eqs. (30) and (46) is related to a state $|\Phi\rangle$ with definite neutrino numbers $N_{\mathbf{p}}$. First of all, note that in a correlator of four neutrino fields

$$\langle \Phi | : \bar{\varphi}^i \chi^j \bar{\psi}^k \omega^l : | \Phi \rangle, \quad (\text{B1})$$

where $i, j, k, l = 1, 2, 3, 4$ are spinor indices, every field operator is a series of the form (14) over the neutrino momentum, i.e., a sum of creation/annihilation operators $\hat{a}_{\mathbf{A}\mathbf{p}}^{(\dagger)}$ with certain coefficients. Therefore, the correlator itself is a quadruple series of quartic expectation values of the form

$$\langle \Phi | : \hat{a}_{\mathbf{A}\mathbf{p}}^{(\dagger)} \hat{a}_{\mathbf{B}\mathbf{q}}^{(\dagger)} \hat{a}_{\mathbf{C}\mathbf{r}}^{(\dagger)} \hat{a}_{\mathbf{D}\mathbf{s}}^{(\dagger)} : | \Phi \rangle; \quad (\text{B2})$$

to prove the theorem, it is thus enough to relate the latter expectation to pairwise contractions of \hat{a}/\hat{a}^\dagger operators. Now, since $|\Phi\rangle$ is characterized by fixed neutrino numbers, the above expectation vanishes unless there are exactly two creation and two annihilation operators amongst the four $\hat{a}^{(\dagger)}$ s and the four momenta match each other, namely, $\mathbf{p} = \mathbf{q}$ and $\mathbf{r} = \mathbf{s}$, or $\mathbf{p} = \mathbf{r}$ and $\mathbf{q} = \mathbf{s}$, or $\mathbf{p} = \mathbf{s}$ and $\mathbf{q} = \mathbf{r}$. If we neglect very ‘‘rare’’ terms with $\mathbf{p} = \mathbf{q} = \mathbf{r} = \mathbf{s}$, then (B2), if it does not vanish, represents an expectation value of a product of two pairs of operators acting in different momentum subspaces, which is a product of two quadratic expectation values,

$$\begin{aligned} &\langle : \hat{a}_{\mathbf{A}\mathbf{p}}^{(\dagger)} \hat{a}_{\mathbf{B}\mathbf{q}}^{(\dagger)} \hat{a}_{\mathbf{C}\mathbf{r}}^{(\dagger)} \hat{a}_{\mathbf{D}\mathbf{s}}^{(\dagger)} : \rangle \\ &\approx \langle : \hat{a}_{\mathbf{A}\mathbf{p}}^{(\dagger)} \hat{a}_{\mathbf{B}\mathbf{q}}^{(\dagger)} : \rangle \langle : \hat{a}_{\mathbf{C}\mathbf{r}}^{(\dagger)} \hat{a}_{\mathbf{D}\mathbf{s}}^{(\dagger)} : \rangle + \langle : \hat{a}_{\mathbf{A}\mathbf{p}}^{(\dagger)} \hat{a}_{\mathbf{C}\mathbf{r}}^{(\dagger)} : \rangle \langle : \hat{a}_{\mathbf{D}\mathbf{s}}^{(\dagger)} \hat{a}_{\mathbf{B}\mathbf{q}}^{(\dagger)} : \rangle \\ &\quad - \langle : \hat{a}_{\mathbf{A}\mathbf{p}}^{(\dagger)} \hat{a}_{\mathbf{D}\mathbf{s}}^{(\dagger)} : \rangle \langle : \hat{a}_{\mathbf{C}\mathbf{r}}^{(\dagger)} \hat{a}_{\mathbf{B}\mathbf{q}}^{(\dagger)} : \rangle, \end{aligned} \quad (\text{B3})$$

where the approximate equality sign refers to the special case with four equal momenta, in which the equality is wrong. Now that we have established such an equality for \hat{a}/\hat{a}^\dagger operators, we can write an analogous expression for the fields

$$\langle : \bar{\varphi}^i \chi^j \bar{\psi}^k \omega^l : \rangle \approx \overline{\overline{\overline{\overline{\varphi}^i \chi^j \bar{\psi}^k \omega^l}}} + \overline{\overline{\overline{\overline{\varphi}^i \bar{\psi}^k \omega^l \chi^j}}} - \overline{\overline{\overline{\overline{\varphi}^i \omega^l \bar{\psi}^k \chi^j}}}, \quad (\text{B4})$$

with a contraction defined as $\overline{\overline{\overline{\overline{\varphi}^i \chi^j}}} \equiv \langle : \bar{\varphi}^i \chi^j : \rangle$. Note that for Majorana neutrinos allowing for coherent neutrino-anti-neutrino mixing, the second term on the rhs may not vanish. Usually, the above expression is written in the form keeping the original order of the four operators, but with an explicitly specified contraction pattern,

$$\langle : \bar{\varphi}^i \chi^j \bar{\psi}^k \omega^l : \rangle \approx \overline{\overline{\overline{\overline{\varphi}^i \chi^j \bar{\psi}^k \omega^l}}} + \overline{\overline{\overline{\overline{\varphi}^i \chi^j \bar{\psi}^k \omega^l}}} + \overline{\overline{\overline{\overline{\varphi}^i \chi^j \bar{\psi}^k \omega^l}}}. \quad (\text{B5})$$

APPENDIX C: NEUTRINO DENSITY MATRIX IN THE FLAVOR BASIS

In the derivation of the effective Hamiltonian (57), the density matrix $\rho_{AB}(\mathbf{p})$ was defined in terms of operators related to neutrino mass states a, b [see Eq. (11)], however, it is often handy to work in the flavor basis instead. Indeed, neutrino flavor currents can be written in terms of a $U(2N_f)$ transformed matrix $\rho_{ff'}^{(\text{fl})}(\mathbf{p})$,

$$\langle \Phi | : \bar{\nu}_f(\mathbf{x}) \gamma_L^\mu \nu_{f'}(\mathbf{x}) : | \Phi \rangle = \sum_{\mathbf{p}} \frac{(1, \hat{\mathbf{p}})}{V} U_{fa}^* U_{f'b} (\rho_{b-,a-}(\mathbf{p}) - \rho_{a+,b+}(\mathbf{p})) = \sum_{\mathbf{p}} \frac{(1, \hat{\mathbf{p}})}{V} (\rho_{f'-,f-}^{(\text{fl})}(\mathbf{p}) - \rho_{f+,f'+}^{(\text{fl})}(\mathbf{p})), \quad (\text{C1})$$

$$\rho^{(\text{fl})}(\mathbf{p}) = \begin{pmatrix} U & 0 \\ 0 & U^* \end{pmatrix} \rho(\mathbf{p}) \begin{pmatrix} U^\dagger & 0 \\ 0 & U^T \end{pmatrix} \equiv \mathcal{U} \rho(\mathbf{p}) \mathcal{U}^\dagger. \quad (\text{C2})$$

Since this transformation is unitary, it induces a unitary transformation of the Hamiltonian $h^{(\text{fl})}(\mathbf{p}) = \mathcal{U} h(\mathbf{p}) \mathcal{U}^\dagger$, and its straightforward application to Eq. (57) yields

$$h^{(\text{fl})}(\mathbf{p}) = \begin{pmatrix} M^{(\text{fl})2}/2|\mathbf{p}| + G_F \sqrt{2} (n_e \mathbb{P}_e^{(\text{fl})} - n_n \mathbb{1}/2) & -i\mathbf{m}^{(\text{fl})} B_\perp(\mathbf{p}) \\ i\mathbf{m}^{(\text{fl})\dagger} B_\perp(\mathbf{p}) & M^{(\text{fl})T2}/2|\mathbf{p}| - G_F \sqrt{2} (n_e \mathbb{P}_e^{(\text{fl})} - n_n \mathbb{1}/2) \end{pmatrix} + \frac{G_F \sqrt{2}}{V} \sum_{\mathbf{q}} (1 - \hat{\mathbf{p}} \cdot \hat{\mathbf{q}}) \mathcal{K}(\rho^{(\text{fl})}(\mathbf{q})), \quad (\text{C3})$$

$$\mathcal{K}(\rho^{(\text{fl})}) \equiv \text{tr}(\rho^{(\text{fl})} \mathcal{G}) \mathcal{G} + \wp^{(\text{fl})\text{diag}} + g_- (\mathcal{U}^* \mathcal{U}^\dagger \wp^{(\text{fl})} \mathcal{U} \mathcal{U}^T)^{\text{diag T}} + g_+ e^{i\Gamma(\hat{\mathbf{p}}, \hat{\mathbf{q}})} \mathcal{G} (\mathcal{U}^* \mathcal{U}^\dagger \wp^{(\text{fl})} \mathcal{U} \mathcal{U}^T)^{\text{offdiag T}}, \quad (\text{C4})$$

where $M^{(\text{fl})2} = U M^2 U^\dagger$, $(\mathbb{P}_e^{(\text{fl})})_{ff'} = \delta_{f,e} \delta_{f',e}$, $\mathbf{m}^{(\text{fl})} = U \mathbf{m} U^T = -\mathbf{m}^{(\text{fl})T}$, and the last term $\mathcal{K}(\rho^{(\text{fl})})$ describes the self-interaction in the flavor basis. One observes immediately that if the PMNS matrix U is real, i.e., no nontrivial CP or Majorana phases are present, $\mathcal{U}^* \mathcal{U}^\dagger = \mathbb{1}$ and the interaction Hamiltonian retains its original, mass-basis form in the flavor basis. In general, however, this is not the case. At the same time, it is interesting to note that in the two-flavor case, $\mathbf{m} = i\mu_{12} \sigma_2$ and the off-diagonal blocks $\wp_{\mp\pm}^{(\text{fl})} = \rho_{\mp\pm}^{(\text{fl})} - \rho_{\mp\pm}^{(\text{fl})T}$ are also proportional to σ_2 , so that simplifications take place when multiplying by the mixing matrix $U = e^{i\theta\sigma_2} \text{diag}(e^{i\alpha/2}, 1)$,

$$\mathbf{m}^{(\text{fl})} = e^{i\alpha/2} \mathbf{m}, \quad (\mathcal{U}^* \mathcal{U}^\dagger \wp^{(\text{fl})} \mathcal{U} \mathcal{U}^T)^{\text{offdiag T}} = e^{i\alpha\mathcal{G}} (\wp^{(\text{fl})\text{offdiag}})^T, \quad (\text{C5})$$

and the remaining Majorana phase α can be eliminated by a gauge transformation (58), i.e., by a rephasing of the two helicity eigenstates. This is how one arrives at a real antisymmetric magnetic moment matrix in Eq. (68) and at a conventional g_+ NSSI term in the self-interaction Hamiltonian (69). Quite naturally, in the three-flavor case, this rephasing is not enough to absorb the two Majorana and one CP phase.

- [1] A. Mirizzi, I. Tamborra, H.-T. Janka, N. Saviano, K. Scholberg, R. Bollig, L. Hüdepohl, and S. Chakraborty, *Riv. Nuovo Cimento* **39**, 1 (2016).
- [2] C. Giunti and C. W. Kim, *Fundamentals of Neutrino Physics and Astrophysics* (Oxford University Press, Oxford, 2007).
- [3] G. G. Raffelt, *Stars as Laboratories for Fundamental Physics* (University of Chicago Press, Chicago, 1996).
- [4] A. Sung, H. Tu, and M.-R. Wu, *Phys. Rev. D* **99**, 121305(R) (2019).
- [5] S. Shalgar, I. Tamborra, and M. Bustamante, [arXiv:1912.09115](https://arxiv.org/abs/1912.09115).
- [6] A. de Gouvêa and S. Shalgar, *J. Cosmol. Astropart. Phys.* **10** (2012) 027; **04** (2013) 018.
- [7] A. Esteban-Pretel, R. Tomàs, and J. W. F. Valle, *Phys. Rev. D* **76**, 053001 (2007).
- [8] Y. F. Li, *Int. J. Mod. Phys. Conf. Ser.* **31**, 1460300 (2014).
- [9] H. Duan, G. M. Fuller, and Y.-Z. Qian, *Annu. Rev. Nucl. Part. Sci.* **60**, 569 (2010).
- [10] L. Wolfenstein, *Phys. Rev. D* **17**, 2369 (1978).
- [11] S. P. Mikheev and A. Y. Smirnov, *Sov. J. Nucl. Phys.* **42**, 913 (1985).
- [12] G. Raffelt, S. Sarikas, and D. S. Seixas, *Phys. Rev. Lett.* **111**, 091101 (2013).
- [13] H. Duan and S. Shalgar, *Phys. Lett. B* **747**, 139 (2015).
- [14] L. Johns, H. Nagakura, G. M. Fuller, and A. Burrows, *Phys. Rev. D* **101**, 043009 (2020).
- [15] R. Glas, H.-T. Janka, F. Capozzi, M. Sen, B. Dasgupta, A. Mirizzi, and G. Sigl, *Phys. Rev. D* **101**, 063001 (2020).
- [16] F. Capozzi, M. Chakraborty, S. Chakraborty, and M. Sen, *Phys. Rev. Lett.* **125**, 251801 (2020).
- [17] H. Duan, G. M. Fuller, and Y.-Zh. Qian, *Phys. Rev. D* **74**, 123004 (2006).
- [18] H. Duan, G. M. Fuller, J. Carlson, and Y.-Zh. Qian, *Phys. Rev. D* **74**, 105014 (2006).
- [19] J. D. Martin, J. Carlson, and H. Duan, *Phys. Rev. D* **101**, 023007 (2020).
- [20] J. D. Martin, S. Abbar, and H. Duan, *Phys. Rev. D* **100**, 023016 (2019).
- [21] A. Mirizzi, *Phys. Rev. D* **92**, 105020 (2015).
- [22] C. Yi, L. Ma, J. D. Martin, and H. Duan, *Phys. Rev. D* **99**, 063005 (2019).
- [23] C. Giunti and A. Studenikin, *Phys. At. Nucl.* **72**, 2089 (2009).
- [24] M. Dvornikov, *Nucl. Phys.* **B855**, 760 (2012).
- [25] V. Cirigliano, G. M. Fuller, and A. Vlasenko, *Phys. Lett. B* **747**, 27 (2015).
- [26] O. Kharlanov and P. Shustov, *EPJ Web Conf.* **201**, 09006 (2019).
- [27] S. Abbar, *Phys. Rev. D* **101**, 103032 (2020).
- [28] T. Ohlsson, *Rep. Prog. Phys.* **76**, 044201 (2013).
- [29] Y. Farzan and M. Tortola, *Front. Phys.* **6**, 10 (2018).
- [30] P. S. Bhupal Dev *et al.*, *SciPost Phys. Proc.* **2**, 001 (2019).
- [31] S.-F. Ge and S. J. Parke, *Phys. Rev. Lett.* **122**, 211801 (2019).
- [32] A. Dighe and M. Sen, *Phys. Rev. D* **97**, 043011 (2018).
- [33] A. Das, A. Dighe, and M. Sen, *J. Cosmol. Astropart. Phys.* **05** (2017) 051.
- [34] Y. Yang and J. P. Kneller, *Phys. Rev. D* **97**, 103018 (2018).
- [35] R. V. Konoplich and M. Yu. Khlopov, *Sov. J. Nucl. Phys.* **47**, 565 (1988).
- [36] P. A. Zyla *et al.* (Particle Data Group), *Prog. Theor. Exp. Phys.* **2020**, 083C01 (2020).
- [37] Z. Maki, M. Nakagawa, and S. Sakata, *Prog. Theor. Phys.* **28**, 870 (1962).
- [38] M. Fierz, *Z. Phys.* **104**, 553 (1937).
- [39] H. K. Urbantke, *J. Geom. Phys.* **46**, 125 (2003).
- [40] B. Dasgupta, A. Dighe, A. Mirizzi, and G. G. Raffelt, *Phys. Rev. D* **78**, 033014 (2008).
- [41] H.-T. Janka, in *Handbook of Supernovae*, edited by A. W. Alsabti and P. Murdin (Springer, Switzerland, 2017), p. 1575.
- [42] M. Th. Keil, G. G. Raffelt, and H.-T. Janka, *Astrophys. J.* **590**, 971 (2003).
- [43] S. L. Glashow, J. Iliopoulos, and L. Maiani, *Phys. Rev. D* **2**, 1285 (1970).
- [44] J. Kneller and C. Volpe, *Phys. Rev. D* **82**, 123004 (2010).
- [45] A. Grigoriev, E. Kupcheva, and A. Ternov, *Phys. Lett. B* **797**, 134861 (2019).
- [46] V. Sadovnichy, A. Tikhonravov, V. Voevodin, and V. Opanasenko, in *Contemporary High Performance Computing: From Petascale toward Exascale*, edited by J. S. Vetter (CRC Press, Boca Raton, 2013), p. 283.